CHALMERS
UNIVERSITY OF TECHNOLOGY

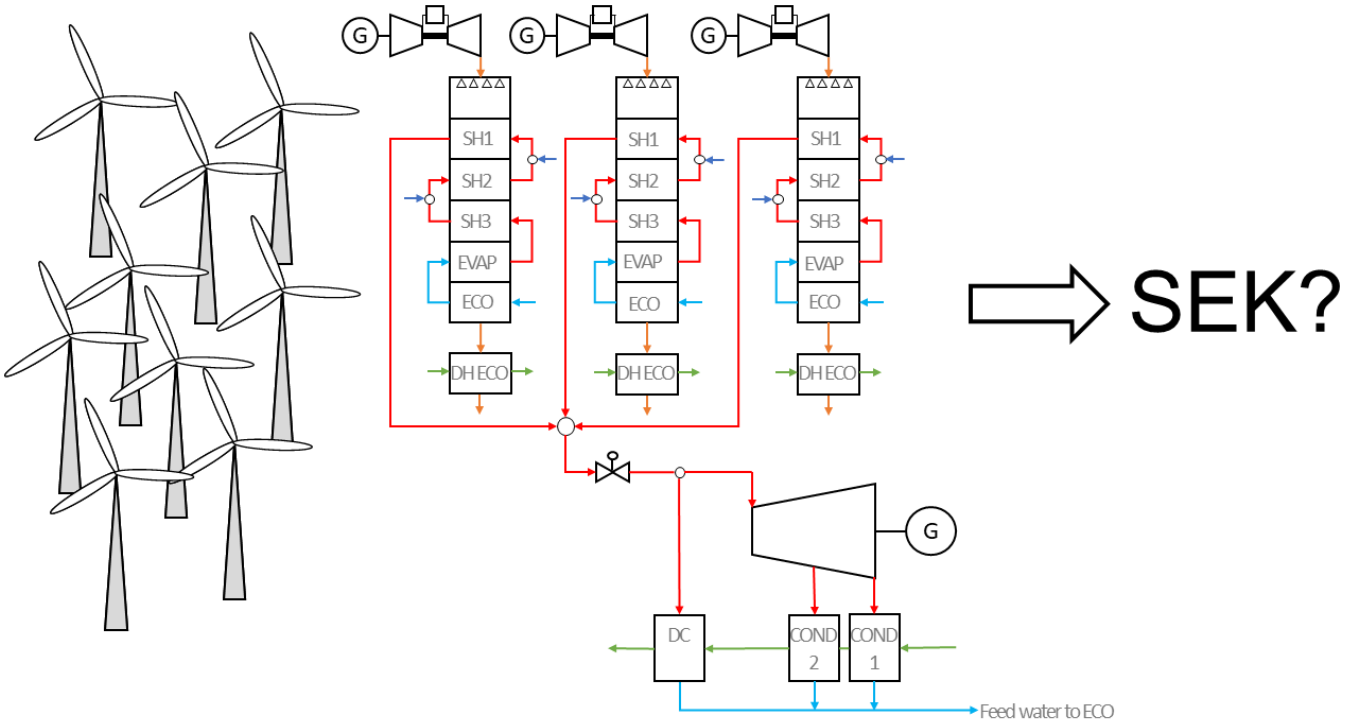


# Opportunities for Flexible Operation of a Combined Heat and Power Plant in Power Systems with Volatile Electricity Prices

Master's thesis in Sustainable Energy Systems

JULIA HANSSON BJÖRCK
LINNÉA ÖSTLUND

Department of Space, Earth and Environment
CHALMERS UNIVERSITY OF TECHNOLOGY
Gothenburg, Sweden 2019

Master's thesis 2019

# Opportunities for Flexible Operation of a Combined Heat and Power Plant in Power Systems with Volatile Electricity Prices

JULIA HANSSON BJÖRCK
LINNÉA ÖSTLUND


CHALMERS
UNIVERSITY OF TECHNOLOGY

Department of Space, Earth and Environment
*Division of Energy Technology*
Chalmers University of Technology
Gothenburg, Sweden 2019

Opportunities for Flexible Operation of a Combined Heat and Power Plant in Power Systems with Volatile Electricity Prices
JULIA HANSSON BJÖRCK, LINNÉA ÖSTLUND



Supervisors:
Ph.D. Candidate Johanna Beiron, Department of Space, Earth and Environment
Dr. Rubén Mocholí Montañés, Department of Space, Earth and Environment

Examiner:
Associate Professor Dr. Fredrik Normann, Department of Space, Earth and Environment

Master's Thesis 2019
Department of Space, Earth and Environment
Division of Energy Technology
Chalmers University of Technology
SE-412 96 Gothenburg
Telephone +46 31 772 1000

Cover: Wind turbines and overall setup of the studied reference CCGT-CHP plant.

Printed by Chalmers Digitaltryck
Gothenburg, Sweden 2019

Opportunities for Flexible Operation of a Combined Heat and Power Plant in Power Systems with Volatile Electricity Prices
JULIA HANSSON BJÖRCK, LINNÉA ÖSTLUND
Department of Space, Earth and Environment
Chalmers University of Technology

# Abstract

To combat climate change, renewable energy sources are preferred in energy systems. Among these are wind and solar, which are characterised by low operational costs and that their energy output depends on weather conditions. The implementation of large amounts of non-dispatchable power generation, that are placed early in the merit order, results in larger and more frequent variations in net power supply in the energy system. This, consequently, leads to volatile electricity prices. For existing power plants to operate profitably in such systems, they need to have flexible operating strategies to profit from high electricity prices. Furthermore, it is preferable to avoid power production during hours with low electricity prices without having to shut down the plant. In this study, a combined cycle gas turbine combined heat and power (CCGT-CHP) plant located in Gothenburg, Sweden has been analysed in order to find profitable operational strategies for scenarios of possible future energy markets.

This study is performed in two steps. In the first, a detailed steady-state process model is derived based on an analysis of historical process data and operating patterns at the reference plant. In the second step, the process model was linearised and implemented into an optimisation model to analyse the CCGT-CHP plant's profitability and operational strat egies in possible future energy systems. Linear equations were derived for power and heat output, as well as fuel consumption, using factorial design and linear regression methods. The equations were validated against process model outputs.

The study concludes that the profitability of flexibilisation measures is highly dependent on the energy system in place. In general, an increased share of non-dispatchable power sources increases the profitability of operating the plant with full steam turbine bypass. This strategy further implies alternative strategies for both gas turbine and supplementary firing operations. However, the optimisation model without the possibility of steam turbine bypass, given historical power market data, proposed a similar operation as the one used at the reference CCGT-CHP plant during the reference year. Nonetheless, fuel taxation and future energy systems could give rise to the need for new operating strategies. If the fuel price is increased, full steam turbine bypass is vital to operate in a profitable manner. That is, operate the plant for heat production. However, for a changed electricity mix in the system, the CCGT-CHP plant could have an important part in the electricity system as well.

# Acknowledgements

We would like to start to extend our deepest gratitude to our supervisors, Johanna Beiron and Rubén Mocholí Montañés, for their tireless support and invaluable inputs throughout the project. We have learned a lot from you! Further, we'd also like to thank our examiner Fredrik Normann for making this thesis possible.

We are grateful to Karl Vilén for his outermost helpful GAMS programming tips and overall code feedback, and we appreciate Göteborg Energi for providing us with process data from their CHP plant. We gratefully acknowledge the support and cheers from Allen (Steve), Hannes, and our families. Thank you for giving us the energy to realise this thesis!

Julia Hansson Björck & Linnéa Östlund, Gothenburg, June 2019

# Contents

# List of Figures

# List of Tables

# Nomenclature

## Abbreviations

| | |
|---|---|
| **CCGT** | Combined Cycle Gas Turbine |
| **CHP** | Combined Heat and Power |
| **COND** | Condenser |
| **DC** | Direct Condenser |
| **DH** | District Heating |
| **DHW** | District Heating Water |
| **ECO** | Economizer |
| **EVAP** | Evaporator |
| **FWT** | Feed Water Tank |
| **GHG** | Green House Gas |
| **GT** | Gas Turbine |
| **HRSG** | Heat Recovery Steam Generator |
| **SF** | Supplementary Firing |
| **SH** | Superheater |

## Variables

| | |
|---|---|
| $\alpha$ | Power-to-heat ratio |
| $\beta$ | Parameter |
| $\dot{m}$ | Mass Flow |
| $\varepsilon$ | Error Term |
| $A$ | Area |
| $C$ | Price |
| $h$ | Hour |
| $L$ | Load |
| $P$ | Power |
| $p$ | Pressure |
| $Q$ | Heat |
| $r$ | Revenue |
| $T$ | Temperature |
| $x_i$ | Design factor |

## Subscripts

| | |
|---|---|
| $in$ | Inlet |
| $out$ | Outlet |
| $s$ | Supply |
| $r$ | Return |
| $amb$ | Ambient |
| $el$ | Electricity |

# 1
# Introduction

## 1.1 Background

The fact that the climate change measured in recent years comes from mankind's exploitation of natural resources is something recognised by nations worldwide [2]. What this climate change actually will result in is highly debated, but studies show that actions need to be taken sooner rather than later to reduce the risk of the catastrophic consequences it could have [2]. Greenhouse gas (GHG) emissions have been identified as one main contributor to the climate change, and one sector that emits large amounts every year is the energy sector [2]. In 2016, electricity and heat generation were responsible for 42 % of the global GHG emissions [3]. In order to reduce these, wind and solar energy can be used for power production purposes. These do not emit GHG during operation, and are resources with potentially large energy outputs [4, 5]. Additionally, seeing as wind and solar energy production barely have any operational cost, they are added in the beginning of the wholesale merit order market in which available energy is ranked based on their operational cost [4]. That is, when there is a lot of wind in the system, the electricity price is reduced and, therefore, the profitability of other power production technologies is reduced [4, 5].

Wind and solar have variable power production and are associated with uncertainties regarding power generation, wind more than solar [5]. From this, in contrast to conventional energy production technologies, the output from variable energy sources is difficult to control [4]. In order to successfully implement such energy resources in the existing system, other plants must be able to respond to the resulting fluctuating net demand of power [4]. A combined cycle gas turbine (CCGT) in a combined heat and power (CHP) context has, with its rather short ramp times, potential for handling fluctuations in electricity net demand [6]. The exhaust from the electricity producing gas turbine is used to drive a steam cycle which produces additional electricity as well as heat in a succeeding steam turbine [7]. However, the change in demand for heat and electricity are not always correlated to one another. For example, when there is a lot of wind power in the system, it might not be profitable to produce electricity in the CCGT-CHP since the operational cost might exceed the electricity price [4, 6]. Nonetheless, the plant is still required to cover the required heat demand. This further adds to the flexibility requirements for these plants; they do not solely need to respond quickly to the fluctuating electricity net demand, but also be able to supply the required heat [6, 8]. In climates found in countries like Sweden, where low temperatures dominate during large parts of year, district heating is an energy efficient way to achieve comfortable indoor climate

[9]. Therefore, many CHP plants in these geographical locations have heat as their primary product [7]. In 2014, Sweden had an installed CHP capacity of 3700 MW for district heating, and 1400 MW for industrial heat demands used in a variety of industrial processes [10].

Variability is, however, not new in these systems, which have always had uncertainties related to the demand-side [5]. This has been in place since the first customer was connected to the grid, and there is therefore a lot of historical data and experience of this variability [5]. Furthermore, the variability on the demand-side can be somewhat predicted based on weekday, time of year et cetera [4]. The current system is, however, not designed to respond to variability and uncertainties on the supply-side to the same extent [4, 11]. In order to understand how current heat and power plants should operate in these changed systems, models and simulations of plants are powerful tools which can be used to analyse how they can be operated and designed to fit the new types of variability arisen from variable renewable resources [11]. Furthermore, analysis of the plants' revenue is an important aspect of how to profitably operate in a system with volatile electricity prices.

## 1.2 Aim and Scope

The aim of this study is to evaluate operational strategies to maximise a CHP plant's revenue in future energy market scenarios. These strategies are compared to the current operation of a reference CHP plant, and an analysis of additional flexibilisation methods is conducted in order to optimise plant operation. By steady-state simulations of a CCGT-CHP plant, and optimisation of operating parameters based on a linearised model formulation, the optimised operating conditions are identified.

The results will ultimately be based on literature, historical reference process data, and steady-state simulations. Therefore, aspects such as process dynamics, maintenance, plant lifetime, and how the strategies would practically be implemented are not part of this study. The focus lies on a plant level and how the CHP is to be operated to maximise revenues, while still fulfilling the district heat demand. The case study questions will be answered using steady-state process modelling, model linearisation, and optimisation, as well as a literature study of additional flexibilisation methods. The overall project method is presented in Section 1.3.

The project's aim is summarised in the following case study questions which are analysed in this report.

- How can an industrial CCGT-CHP plant be modelled, linearised, and optimised to maximise plant revenue?
- What are the optimal operational strategies for a CHP plant? How does the current operation of the reference plant differ from these?
- How will future electricity markets, with volatile electricity prices, impact the operational strategies of a CCGT-CHP plant?
- How will flexibilisation alternatives such as thermal storage and a direct condenser affect the operation of a CCGT-CHP plant?

## 1.3 Overall Project Method

The project's overall method is illustrated in Fig 1.1, where results from previous parts are inputs to the succeeding ones. The figure shows how the different steps, yellow boxes, lead to the overall aim of the project, green box.

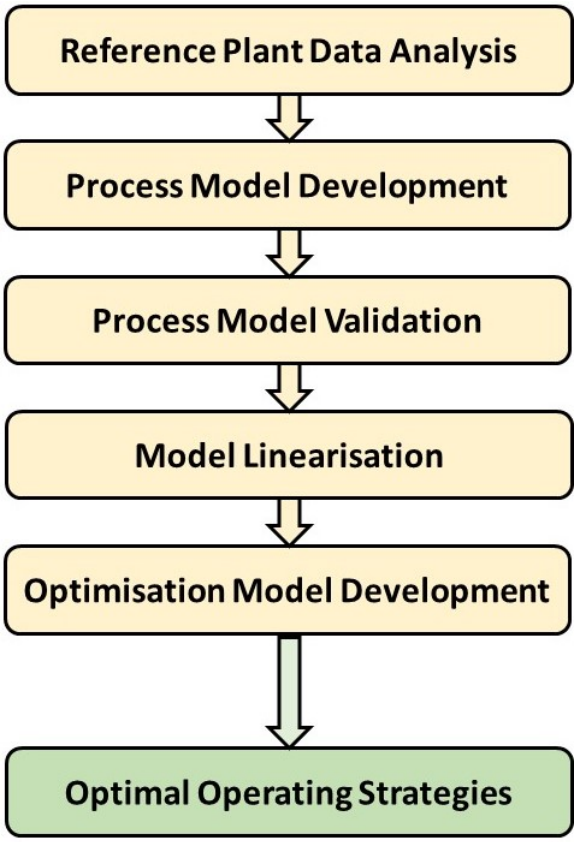


**Figure 1.1:** General project method, yellow boxes, to find optimal operating strategies, green box, for the reference CHP plant.

The basis for this study is hourly process data and production data from the reference plant. This data is analysed in Excel in order to identify which operating strategies have been used during the reference year, 2016. These, as well as detailed process data regarding the plant's operating conditions, such as temperatures and pressures, are used to develop steady-state process models, both design and off-design, of the plant in the commercial software EBSILON®Professional. The developed process models are validated against historical process data to ensure their accuracy. Thereafter, parameters which highly influence the plant's power and heat output, as well as fuel consumption, are to be identified. These are translated into equations using the linearisation methods factorial design and linear regression. The linear equations derived in Excel are to be validated against the process model to evaluate their accuracy in predicting the process' behaviour. Once the linearised equations are validated, they are used to develop an optimisation model in the commercial programming software GAMS, which is designed to maximise the plant's revenue. Simulations are conducted with the optimisation model in order to find

profitable operating conditions, which are compared to historical plant operations. Furthermore, simulations are run in order to analyse how possible future energy markets affect the plant's operations and revenue.

This report starts with two theory chapters; one analysing the systems in which the plant operates, followed by one presenting a technical description of a CCGT-CHP plant. In addition, the latter includes the identified historical operational strategies at the reference plant. Thereafter, the report's structure follows the work flow presented in Fig 1.1, where each step is treated in its own chapter. Each chapter includes a theory section, a method section, and the step's results. The overall case study results are presented and discussed in an individual chapter followed by the conclusions drawn from the study.

# 2
# Power and Heat on a System Level

Since the studied reference plant is a heat and power plant, it operates on two markets; the electricity market and the district heating market. To find profitable operating strategies for the plant, the systems in which the plant operates are important to evaluate. This chapter describes the electricity and district heating markets on a system level.

## 2.1 Power Production

In the modern society of today, electricity is something taken for granted. Whenever wished for, lamps are turned on instantly by just the push of a button [12]. All advanced equipment and tools used in everyday life entirely rely on electricity in order to function. Thus, electricity is a foundation for the modern society, which sets requirement on an instant and fast responsive supply. The increasingly advanced society and the electricity demand is expected to continue to grow and expand [12, 13, ch.1]. Since electricity is an instant energy source, with limitations on acceptable storage capabilities, a balance between supply and demand is essential. To achieve this, demand-side management and response can be implemented as well as increasing flexibility of individual plants [4, 5]. When more non-controllable low-cost power sources enter the market, the need for flexible power production techniques increases as one approach to meet this altered power system [5]. Flexibility of a power plant relates to its ability to make fast responses to a fluctuating net demand to ensure a reliable supply [4].

There are three parameters that characterise the flexibility of a thermal plant: minimum load, start-up time, and ramp rate [4]. The minimum load is the lowest net power output from a plant at stable operating conditions [4]. It is desirable to have a low minimum load as expensive start-ups can then be avoided [4]. However, part load operation is usually related to decreased plant efficiencies and might require the use of supplementary firing to be stable, further decreasing the efficiency [4]. To have a short start-up time increases the flexibility as the plant can react to a demand-change more rapidly [4]. A fast start-up time is, however, related to an increased thermal stress of the equipment which reduces its life time [4]. Lastly, the ramp rate defines how fast a change in new power output during operation can be obtained [4]. The configuration of a combined cycle gas turbine (CCGT) plant enables a rather fast response to changes in the power market [14]. In order to fully utilise the flexibility, the plant has to be well-designed, which in this context implies a short start-up time, fast ramping capability and an efficient part load operation [14]. Accurate forecast possibilities are further an important aspect in order to be

able to utilise a flexible configuration [14].

### 2.1.1 Electricity Markets in Sweden

The main sources for power production in Sweden during one year is shown in Fig 2.1. As illustrated in the figure, nuclear power stands for a large share of the power production in Sweden, where hydro is used to regulate the supply. Nuclear and hydro power stands for 80 % of Sweden's power production, and about 10 % comes from wind and CHP each [10]. Thermal power sources including CHP from industry, district heating, conventional power, and gas turbines [10].

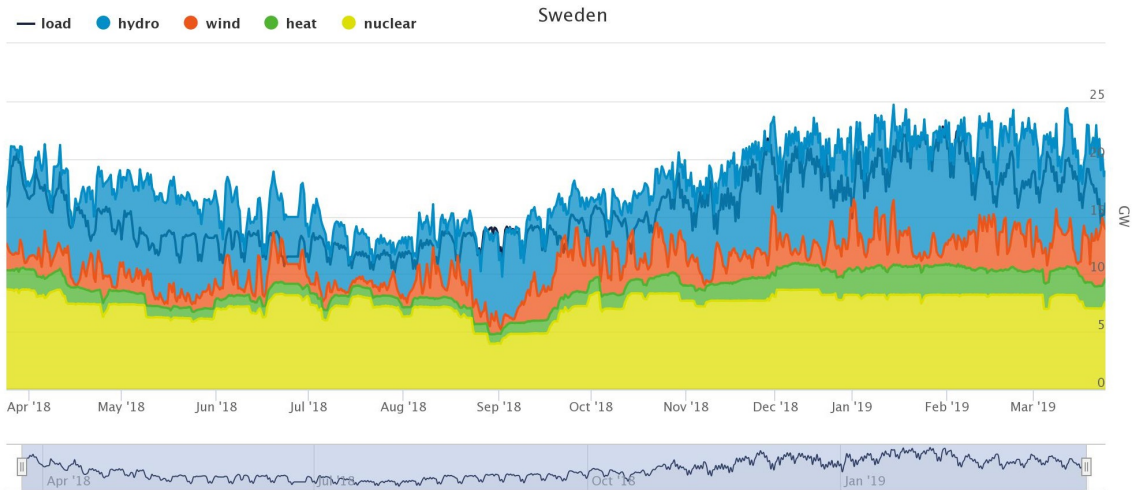


**Figure 2.1:** Electricity production mix in Sweden, March 2018-March 2019. The black line represents the system load [15].

The electricity market in Sweden is a liberalised one, where the current price is based on supply and demand in a day-ahead market. The utilisation of each technology, and therefore electricity price, is dependent on the merit order of the available power technologies [5]. The principle of merit order is illustrated in Fig 2.2. By ranking the available power production technologies based on their variable cost, from smallest to largest, the last unit to be used sets the electricity price [4]. That is, the technology intersected with the demand-curve, black line in Fig 2.2.

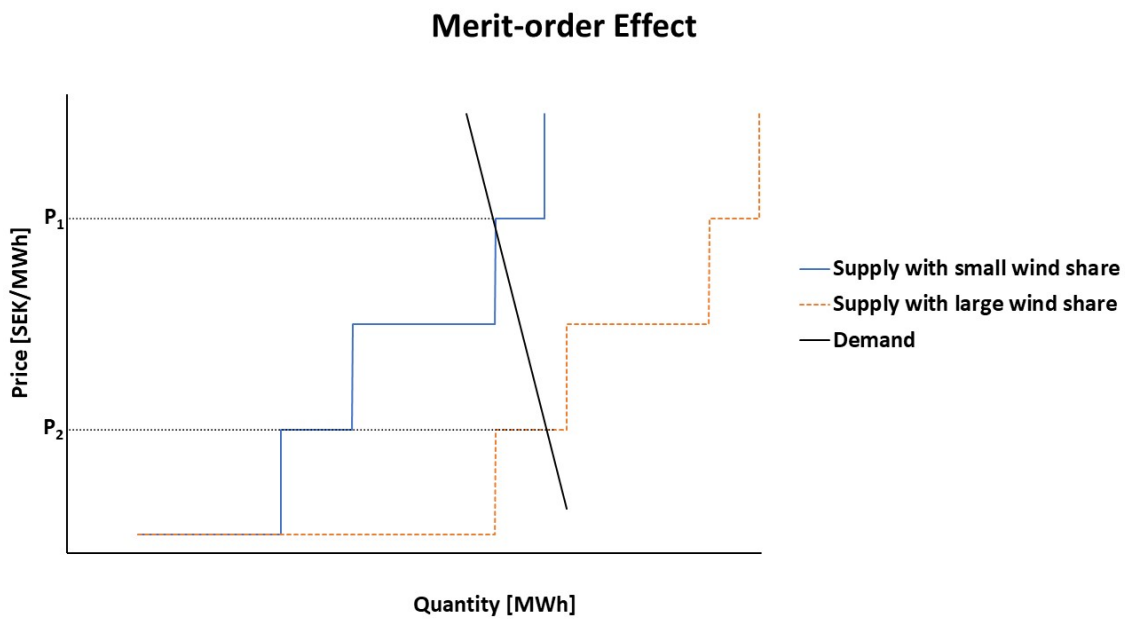


**Figure 2.2:** Merit order with and without wind power in the electricity system. The marginal electricity cost, P, is shown for both cases.

The variable cost of a plant is set by several factors, such as fuel price and emission costs [4]. For example, since the operating cost of nuclear power is low and is not associated with $CO_2$-emissions, it is used as base load and is operated throughout the year [4, 15]. Furthermore, wind and solar power production have marginal variable cost related to them, why they are integrated at the beginning of the merit order once available. This will consequently push other technologies further out in the merit order [4, 5], illustrated by the orange line in Fig 2.2. The electricity price when there is a small amount of wind power in the system, $P_1$, is larger than for periods with a large share of wind, $P_2$. Furthermore, adding or increasing $CO_2$ and energy tax to the system will ultimately increase the operational cost for fossil fuel plants, and push them further out in the merit order [5]. Thereby, times for profitable operation of such plants are reduced significantly, which becomes apparent at larger wind power penetration levels [5].

Wind and solar are variable power sources and do not react to a demand-side change, as they are solely weather dependent. When increasing the share of these types of technologies in the energy system, the need for flexibility from other power production technologies increases [4]. A technology with flexibility is a CCGT-CHP plant. In the merit order, gas turbines belong to the category of technologies which are turned on last, making them operate at peak loads and as stand-by due to their relatively high variable cost. In Sweden, when gas turbines are utilised in a combined cycle, they have a higher prioritisation in order to also fulfil the heat demand [10]. CHP plants are, however, often operated in a heat-controlled mode, where the need for district heating sets the plant load [4]. Therefore, their ability to respond to an increased power demand is somewhat limited [4].

## 2.2 District Heating System

District heating systems are found all over the world in regions with low temperatures during a large part of the year, where the main user categories are buildings and industries [16]. In a district heating system, heat is provided to the users in the system, rather than each user produces its own heat, and it is distributed through underground piping from a centralised heat production source [17]. In Scandinavian countries, up to 90 % of the central city areas are supplied with district heat [9]. Due to the development of building technologies, the need for district heat will decrease once low-energy buildings are in place [18]. However, since the majority of existing buildings will not be replaced by low-energy alternatives in the near future, district heating will remain essential [18].

The use of district heating systems is often related to lower $CO_2$-emissions than when individual electric heating of buildings are used [18]. Furthermore, the central idea of district heating systems is to reduce the amount of primary energy, which is realised through a higher energy efficiency by utilising heat recovery [9]. The design of a district heating system varies depending on the local and excess heat resources, including CHP, waste-to-energy, and waste heat from industrial processes [16]. Additionally, producing heat from a centralised CHP plant can make it easier to produce heat from renewable resources compared to heat production in individual residential buildings [17]. When operating a CHP plant, large amount of waste heat from power generation is utilised, and fuel efficiencies over 90 % can be achieved [17].

### 2.2.1 District Heat Market in Sweden

In the district heating system in Sweden, there are large seasonal load variation as well as variations on a daily basis [19]. The seasonal variations are mainly a result from varying outdoor temperature, whereas daily variations can be a result from customer social behaviours [19]. One example is the consumption of hot water in residential areas which varies during a day [19]. Due to these variations, there is a need for flexibility in a district heating system, which in Sweden can be realised by CCGT-CHP plants [20]. Waste heat from industrial plants and heat from waste incineration are prioritised and utilised when available to reduce energy loss in a cost efficiency manner [20].

Compared to the fluctuating electricity prices, the price for district heating does not vary to the same extent. Many district heating companies, including the company providing district heating at the location studied in this project, utilises seasonal consumer pricing, with one price for winter, summer, and autumn/spring, respectively [21, 22, 23].

# 3

# Combined Heat and Power Plant Operation

In this chapter, technical descriptions of the plant's units are included as well as a study of a set of flexibilisation measures. This background is later used when deriving process models of the plant. The chapter also includes an overview of the reference plant's setup together with findings from a data analysis of historical operating data from the reference plant.

## 3.1 CCGT-CHP Technology

CCGT-CHP is a type of CHP production technology. In general, it consists of a power producing gas turbine together with a heat recovery steam generator, HRSG, and a steam turbine equipped with a condenser [24], see Fig 3.1 The gas turbine's exhaust gases are heat exchanged in the HRSG to produce high pressure and temperature steam [24]. The steam enters a steam turbine where additional electricity is produced, and it is thereafter condensed to produce heat to a heating system [24].

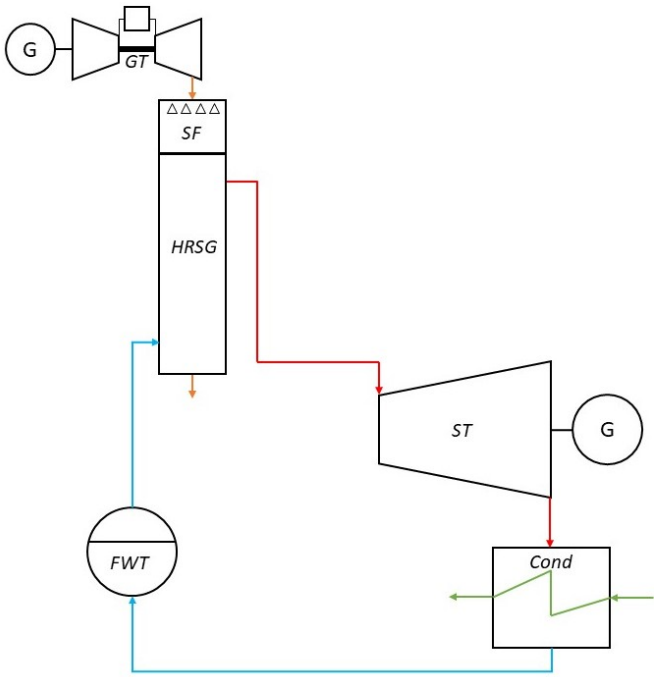


**Figure 3.1:** Schematics of a combined cycle CHP plant with a gas turbine, HRSG equipped with supplementary firing (SF), steam turbine (ST), condenser (Cond), a feed water tank (FWT), and a generator (G).

The ratio between the produced power and heat, $\alpha$, describes how much power is produced at a given unit of heat [7]. See Eq 3.1, where $P$ is the produced power and $Q$ the produced heat. $\alpha$ can be adjusted to meet the demand of each product, and is therefore an essential operational parameter for CHP plants.

$$\alpha = \frac{P}{Q} \tag{3.1}$$

Overall, a CCGT plant consists of two thermodynamic cycles; Joule-Brayton for the gas turbines and a Rankine-cycle for the steam cycle [7, 24]. In the Joule-Brayton cycle, air is compressed, heated in a combustion chamber, and expanded in a turbine where electricity is generated. The exhaust gases leaving the turbine have a temperature of approximately 450-650 °C, which implicates low efficiency if not utilised. To increase plant efficiency, the exhaust heat is used in the HRSG, to further produce both electricity and heat. If a larger plant output is required, supplementary firing (SF in Fig 3.1) can be utilised to increase the temperature of the exhaust gases, and, thereby, the plant output [24].

The units in a combined cycle gas turbine (CCGT) plant are described in detail in the sections below.

### 3.1.1 Gas Turbine

The main objective for a gas turbine in a CHP plant is power production. Gas turbines can utilise a wide range of fuels, from gas mixtures to crude oils [24]. However, burning unclean fuels, such as heavy oils, requires frequent maintenance and often fuel pre-treatment to avoid corrosion and ash deposits, thus natural gas is a common fuel used for gas turbines [24]. Additionally to fuel type, there are a wide range of parameters that influence the output of the gas turbine and, consequently, any connected cycles [14]. For example, ambient ingestion temperature, pressure and humidity are parameters that, apart from gas turbine load, affect the exhaust gas temperature and flow from the turbine [14].

For gas turbines in a combined cycle context, it is essential from an efficiency aspect to maintain the live steam temperature [25]. It is thus desirable to maintain a high exhaust gas temperature even if the power output is decreased. This is realised by reducing the fuel supply and reducing the compressor air flow via variable inlet guide vanes [25]. Equivalent part load behaviour can be achieved through reducing the rotational speed, which enables electricity production at the grid's frequency [25].

The gas turbine output will decrease the more it is operated due to degradation of equipment [14]. Degradation mainly occurs by fouling and ageing, where the first is recoverable whereas the second is a non-recoverable event and needs equipment replacement to realise full performance [14, 26]. Fouling, especially in the compressor, arises from air ingested from the environment, where particles cause pressure drops in the air intake system. The pressure drops will result in performance losses and thereby reduce the output from the gas turbine [26]. This can partly be prevented

by installing air filters in the air ingestion system and by frequent maintenance of the equipment [14]. On the other hand, equipment cannot be recovered after ageing, but the use of clean fuels is one proactive action that limits the ageing rate [26]. After 8000 operating hours with a rather clean fuel, the output of a combined cycle is reduced by 0.8-1.5 % due to the compressor's ageing. Furthermore, turbine fouling, which arises from the ashes formed in the combustion process, is not substantial when burning a clean fuel such as natural gas [14, 26].

### 3.1.2 Heat Recovery Steam Generation

An HRSG utilises the heat in the gas turbine's exhaust gases in order to produce high pressure and high temperature steam [24]. If the steam is to be used in a steam turbine, the turbine sets the requirements for pressure and temperature in the live steam flow [24]. An HRSG usually consists of economisers for feed water preheating, evaporators with a steam drum and superheaters. These units are heat exchangers with water/steam inside the tubes, and counter-currently flowing flue gases on the tube outside [14]. As the heat transfer is lower for the exhaust gases, finned tubes are usually installed to increase the heat transfer area. The exact HRSG design differs depending on the plant's applications and requirements [24].

For a given set of steam properties and demand from the steam turbine, there are efficiency losses associated with large flue gas temperature and flow [14]. On the other hand, with large flue gas flow and temperatures, the possibility of producing high quality steam is increased, which can be realised using supplementary firing [24]. The minimal temperature difference between the two streams is called the pinch point, which, with an energy optimisation approach, should be small in order to produce as much steam as possible [14, 24]. By optimising the HRSG design and flue gas flow, exergy and energy losses can be minimised [24]. As the HRSG is the link between the gas turbine and the steam turbine, it has to adapt to load variations and the short start-up times of the gas turbine. This sets requirements of the HRSG design, which must be available and reliable [14].

During part load operation, there is a risk of steam production in the feed water economiser which reduces the HRSG performance [14]. In order to avoid this, the economiser is designed to produce sub-cooled water at the outlet [14]. To further reduce the risk of evaporation in the economiser, a valve can be installed downstream [14]. This enables feed water preheating at higher pressures, where the temperature of evaporation is higher compared to the evaporator. Thereby, the feed water heating is realised without evaporation, and the stream is throttled to the desired pressure before entering the evaporator.

### 3.1.3 Steam Cycle

A steam cycle operates according to the thermodynamics of a Rankine cycle [12, Ch.4]. Depending on plant application, different steam turbine configurations are suitable. For a plant with heat as its primary product, a back-pressure turbine is

appropriate, whereas a condensing turbine is preferable for electricity production purposes [24]. The pressure out of the last turbine stage, the back pressure, is restricted by the temperature of the cooling medium [27]. When producing district heating water (DHW) with the turbine outlet steam, the target temperature of the DHW determines the back pressure [27, 28]. In this application, it is favourable to utilise two condenser and realise the final temperature increment of the DHW with a steam extraction [27, 28].

By increasing the temperature in multiple condensers, exergy losses are reduced since more energy can be produced in the turbine, generating more valuable work compared to heat [28]. Both the return and the supply temperature of the DHW will impact the performance of the steam cycle. Lower return temperature implies a lower condensing pressure in the first condenser and thereby an increased electricity production [28]. For a higher supply temperature, the condensing pressure in the second condenser increases, which in turn drives more steam through the last turbine stage and, thereby, through the first condenser [28]. Therefore, pressure control of the steam turbine outlets is vital to ensure the required supply temperature [27].

### 3.1.4 Control Strategies

In a heat and power production plant, control structure and strategies play a crucial part during operation. Two vital control strategies in a CCGT-CHP plant are described below.

#### 3.1.4.1 Live Steam Pressure Control

In a CCGT-CHP plant, the live steam pressure is the pressure of steam leaving the last superheater in the HRSG. The steam is to enter the steam turbine, and the turbine inlet pressure can be controlled by valve throttling or the use of sliding pressure [29]. When operating in sliding pressure mode, the pressure in the HRSG is controlled by the steam turbine to be approximately the same as the turbine inlet pressure. The turbine inlet control valve is constantly kept fully open, even when the steam mass flow varies. A central concept in sliding pressure control is the steam turbine's swallowing capacity, which is determined by the turbine's geometry [29]. The aim is to satisfy the swallowing capacity by keeping the volumetric flow through the turbine constant, regardless of the steam mass flow. In a CCGT-CHP, the mass flow of steam varies depending on the gas turbine load. The fixed volumetric flow is realised by controlling the steam pressure to be reduced when reducing gas turbine load [14]. Otherwise, at part load operation of the gas turbine, the steam generation would decrease if the nominal pressure was to be maintained. By controlling the pressure to fulfil the swallowing capacity, the steam production will increase due to the decreased pressure [29].

One alternative to sliding pressure operation is the use of valve throttling [29]. With this method, the swallowing capacity of the steam turbine is achieved by a control valve before the turbine inlet [29]. The valve is controlled to throttle the steam flow to ensure a relatively constant volumetric flow to the turbine [29]. That is, the

steam turbine does not determine the HRSG-pressure, which instead is set mainly by the gas turbine load. For part load operation, the live steam pressure is held constant but since the mass flow is decreased, the steam is throttled before entering the turbine to ensure the nominal volumetric flow [29]. This, in turn, generates a smaller enthalpy drop over the steam turbine and thus a lower efficiency compared to the utilisation of sliding pressure [29]

In contrast to valve throttling, sliding pressure has a higher heat recovery in the HRSG, produces more steam and eliminates both throttling and efficiency losses in the steam turbine control valve. This, altogether, increases the efficiency and power output of the combined cycle [29]. However, sliding pressure is associated with high HRSG pressure drops and a complex operation of the HRSG due to the interconnections with the steam turbine [29]. Nonetheless, using sliding pressure is generally more favourable from an economical perspective compared to valve throttling since the thermal efficiency can be maintained even at part loads [14, 29].

#### 3.1.4.2 Live Steam Temperature Control

In a CCGT-CHP, the high temperature exhaust gas is used to produce high temperature steam. However, if the temperature of the steam is not controlled, there is a risk of damage on the superheater's tubes [14]. To avoid this, the superheating part of the HRSG can be divided into sections with feed water injections, called an attemperator system [14], see Fig 3.2. The injection of high-pressure feed water ensures that the steam temperature does not exceed material limitations. Injections are made after each superheater to cool the steam to the acceptable temperature [14].

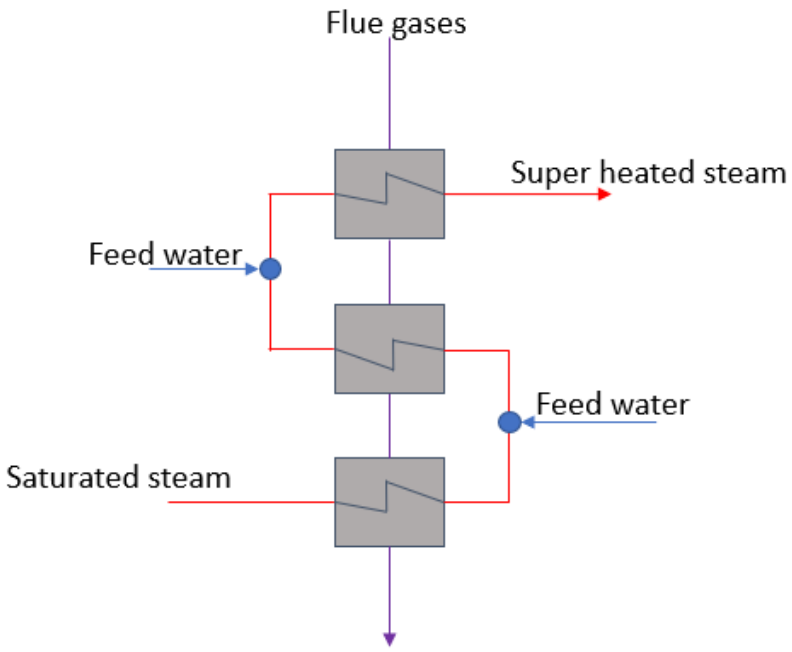


**Figure 3.2:** Schematic set-up for superheaters equipped with an attemperator system.

## 3.2 Flexibility Measures of a CCGT-CHP Plant

Since a CHP plant produces both heat and power, and the demand for these can vary independently, product flexibility is vital to meet the respective demands [4]. In addition to varying the power-to-heat ratio, some additional flexibilisation measures for CHP plants are presented in the following sections.

### 3.2.1 Thermal Storage

In a CHP plant, heat is usually the output that controls the plant operation, which thereby limits the opportunities for balancing power demand [4]. This partly disables operational strategies based on electricity prices, which would be favourable in a power system with large penetration of renewable power production [4]. A large renewable power generation, and the inability to reduce the CHP plant's power production due to a heat demand, lead to a nearly inevitable curtailment of renewable energy [30]. However, as thermal heat storage makes it easier for CHP plants to adapt to demands from both heat and power markets, it facilities a strategical incorporation of both high renewable energy production and CHP plants [30].

By implementing a thermal storage tank to a CHP plant, the heat and power production can partly be decoupled and thereby increase the plant's operational flexibility [4]. The use of a thermal storage tank increases the income due to the possibility of producing electricity during spot price hours and avoiding generation during low price hours [31]. The decoupling is realised by the ability to store surplus heat produced during periods with high electricity prices and low heat demands [4]. On the contrary, when the penetration of renewable power is large, i.e. electricity price is low, a thermal storage discharge can be used to fulfil the heat demand. Thereby, having no or very low plant generation at unprofitable operating hours [4]. Thus, the incorporation of a storage tank enables large penetration of renewables, i.e. less curtailment, while fulfilling the heat demand. By discharging the heat during demand peaks, it is further possible to avoid starting expensive back-up heat generating plants [31].

### 3.2.2 Operational Strategies

Flexibility of a CCGT-CHP can be realised through equipment installations such as duct burners for supplementary firing but also via the configuration of the plant. Having several gas turbines with individual HRSG lines producing steam to a single steam turbine will enhance the flexibility of the plant [7, 14]. The load can be balanced over several gas turbines and gives the possibility of operation across a wider load range [32]. It further decreases the demand response time of the plant, due to the increased ramping rate that can be achieved [32]. Since all gas turbines ramp up in parallel, full plant load can be obtained relatively quickly compared to having one large gas turbine ramping up [33]. Several gas turbines in parallel will also increase the plant's part load performance [7]. However, as part load is associated with lower efficiencies, it is often preferable to have several small gas turbines oper-

ating at their full loads, rather than one large mainly operated at part loads [7, 32]. That is, utilising the fact that equipment efficiency is highest at nominal loads. An increased part load performance will in turn reduce the operational expenses since the heat and power output per unit of fuel is increased [14, 32].

Several gas turbines in parallel enables maintenance without shutting down the whole plant, thereby avoiding revenue losses [32]. With this configuration, sequential maintenance can be performed and still ensure fulfilled power and heat demands [32]. However, frequent start-ups and ramping causes thermal stress to the equipment which in turn requires maintenance [4, 32]. This will increase the operational costs of the plant, but these are compensated for in the ability of sequential maintenance where total power station outage is avoided [32].

For CHP plants, the power-to-heat ratio further realises operational flexibility. In cases where large amounts of electricity are required, the power-to-heat ratio is increased as much as possible by expanding the steam in the steam turbine [7]. When heat is the main product, the steam can either be extracted at a high pressure, corresponding to a high temperature, or even bypass the steam turbine to directly condense and exchange heat with the heating system, i.e. producing less power and more heat [7]. In addition, having bypassing over the different pressure levels in the steam turbine can further increase the plant's operational flexibility as altering over a wider range of $\alpha$-values is enabled [34].

### 3.2.3 Supplementary Firing

The exhaust temperature from the gas turbine limits the steam production and thereby the plant's heat and power production [12]. To be able to increase these outputs, supplementary firing, realised through duct burners, can be utilised before the HRSG to increase the flue gas temperature [14]. Additional fuel, usually natural gas, is supplied in the burners and since the turbine exhaust gases contain, at least, 50 % air, no combustion air is required [12, 35]. However, the maximum firing potential in the duct burner is limited by the amount of oxygen in the exhaust gases [14].

Since the plant's fuel consumption is increased, the utilisation of supplementary firing usually lowers the plant efficiency [12, 14]. Nonetheless, its operational flexibility makes it suitable for cogeneration plants, since it enables individual control of power and heat respectively [12, 14]. Supplementary firing might also lower the pinch point, which can increase the steam production and thereby the power output from the plant [14]. The result can thus be an efficiency increase despite the increased fuel consumption [14].

## 3.3 Reference Plant Setup

The overall configuration of the reference CCGT-CHP plant is illustrated in Fig 3.3. It consists of three parallel SGT-800 gas turbines, with individual HRSGs.

Each HRSG contains three superheaters (SH1-SH3), an evaporator (EVAP), a feed water economiser (ECO), and a district heat economiser (DH ECO). The steam generated in the HRSGs is mixed before entering the steam turbine. The plant is equipped with two condensers (COND 1 and COND 2), which heat the DHW. It is also equipped with a direct condenser (DC) to be used for steam turbine bypass. From the condensers, the feed water enters a feed water tank, which provides the HRSG with subcooled feed water.

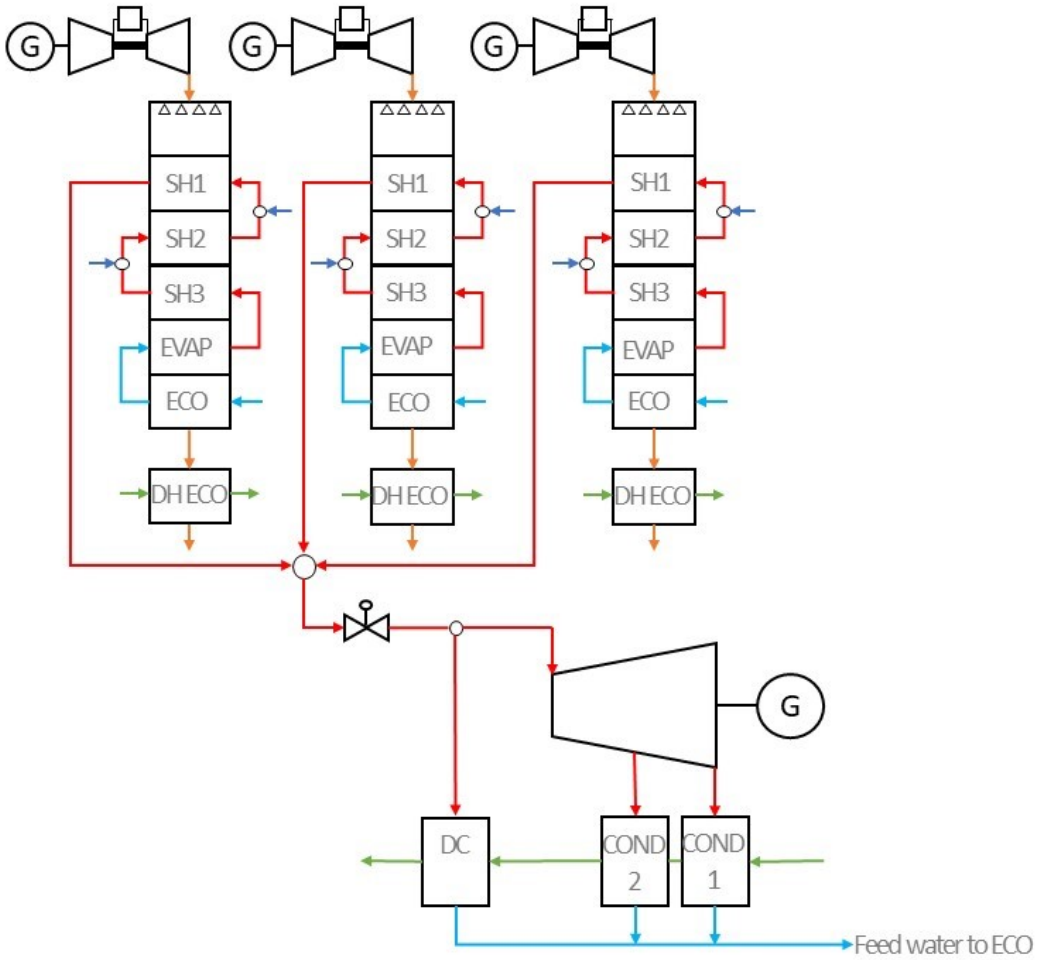


**Figure 3.3:** Schematics of the reference process with three gas turbines, HRSG equipped with supplementary firing, steam turbine, a direct condenser (DC), and two condensers (COND 1 and COND 2). Each HRSG consists of three superheaters (SH1-SH3), an evaporator (EVAP), a feed water economiser (ECO) and a district heat economiser (DH ECO). The live steam temperature control is realised with feed water injection before SH1 and SH2, which is illustrated in the figure with dark blue arrows.

The reference plant has the possibility of operating with sliding pressure, but it generally utilises valve throttling as pressure control strategy. Furthermore, live steam temperature control is applied, which is illustrated with the dark blue arrows before SH1 and SH2 in Figure 3.3.

### 3.3.1 Data Analysis - Identified Historical Operations

During 2016, the reference plant was in operation during the period January-April and November-December.

By studying the reference plant's historical operating data from 2016, it can be seen that the gas turbines were operated either at full, half or no load. This is illustrated in Fig 3.4, which shows the gas turbines' power output from January to the middle of April. The same trend applies for the period November-December.

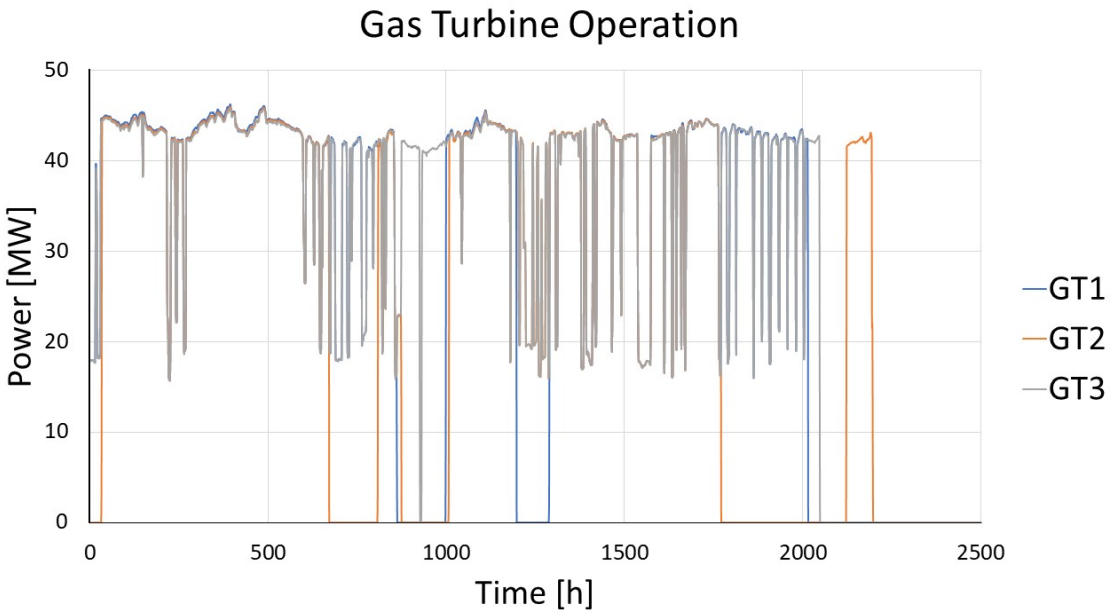


**Figure 3.4:** Reference plant's gas turbine power output during January-April 2016.

It was identified that when the plant is in operation, the gas turbines are operated at full loads, above 85 %, more than 87 % of the time. Full gas turbine power output varies depending on ambient temperature, thus loads above 85 % were considered as full gas turbine operation. The remaining 13 % was operated at part loads, 40-60 %.

The overall trends in the reference plant data show the following operational strategy when going from no to full gas turbine load, also presented in Fig 3.5. First, one gas turbine is operated at part load. To increase the output, a second gas turbine is turned on and operated in part load. To further increase the output, one of the operated gas turbines is ramped up to full load, followed by the second gas turbine previously operated at part load. In order to additionally increase the output, the third gas turbine is turned on and operated at part load, which then can be increased to full load. In general, it is first when all three gas turbines are operated at full load that supplementary firing is utilised if an increased plant output is required. Thus, the strategy utilised at the reference plant enables flexible operations.

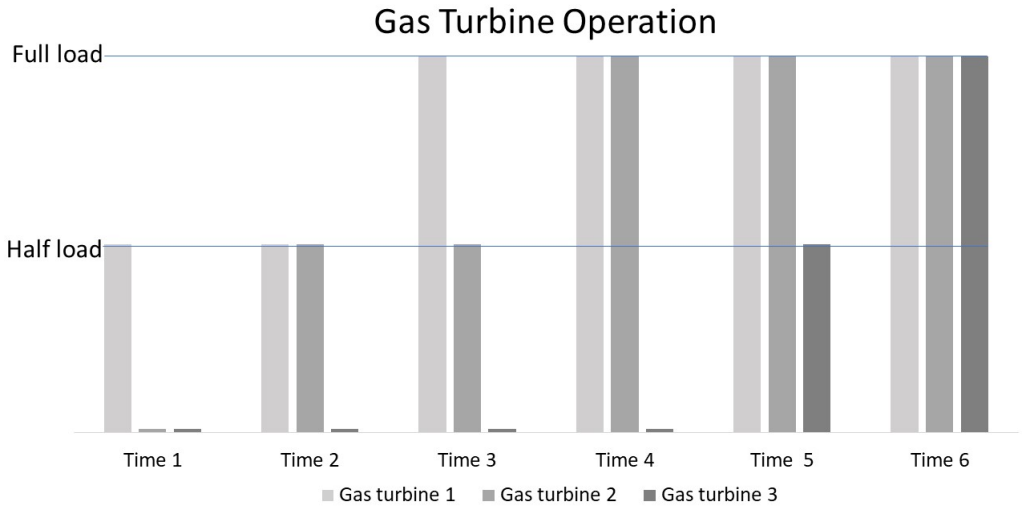


**Figure 3.5:** Operational strategy from zero to full gas turbines output.

The historical data from the reference plant reveals that when supplementary firing is used for one gas turbine line, it is used for all gas turbines operated at that time. This is illustrated in Fig 3.6, where the use of supplementary firing in January 2016 is plotted. The figure shows that the three supplementary firing combustors are always operated simultaneously with the same load. Furthermore, 98 % of the time that supplementary firing was utilised, all three gas turbines were operated.

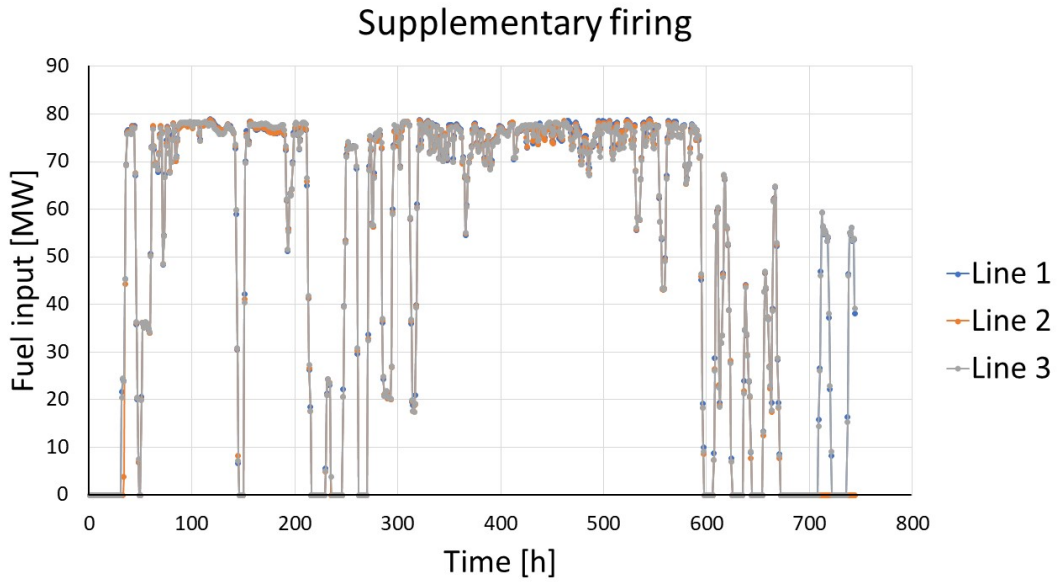


**Figure 3.6:** Historical operating trends for supplementary firing in the three HRSG lines.

That supplementary firing is only used for gas turbines running at full load can be shown by sorting the historical data based on gas turbine load, and analyse the use of

supplementary firing at each point. This is illustrated in Fig 3.7. The dots represent the load of supplementary firing, and the duration curve for gas turbine output is shown. For gas turbine loads below full load, i.e. 40 MW, the supplementary firing loads are constantly zero.

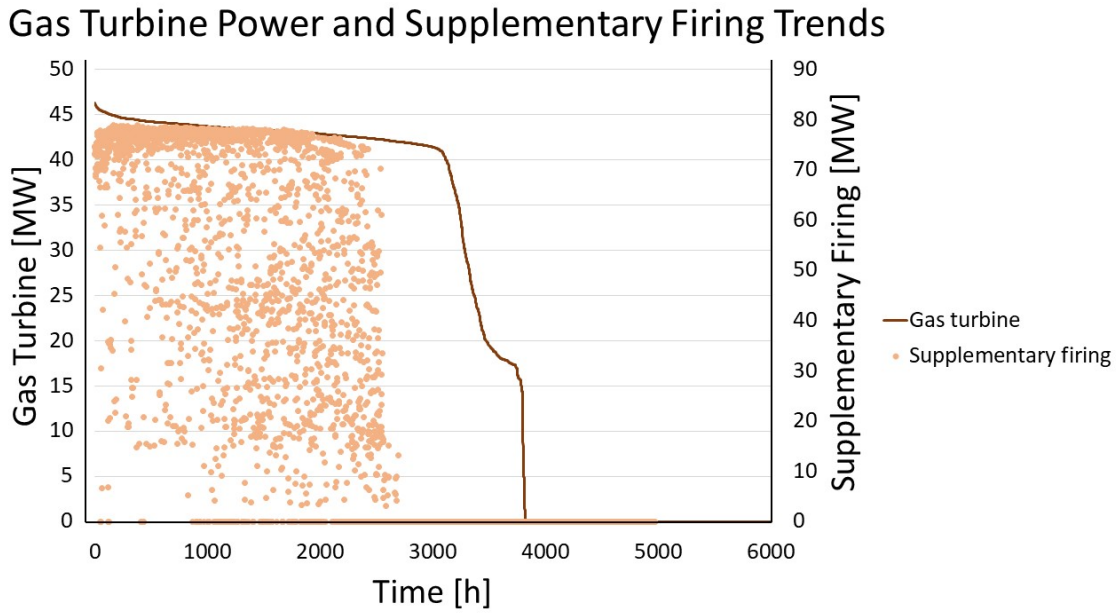


**Figure 3.7:** Duration curve for gas turbine operation with supplementary firing load. The dots correspond to supplementary firing load and the red line size ordered loads for one gas turbine.

The historical data further revealed that the plant operates with only two lines for about 10 % of the year, and operation with only one gas turbine occurred less than 1 % of the year.

# 4
# Process Modelling

To find optimal operating strategies for the reference CCGT-CHP plant, process models of the plant were created to analyse how the plant operates. This chapter starts with a theoretical background to modelling considerations, followed by the modelling methods used in this study as well as the resulting process models.

## 4.1 Theory - Modelling Considerations

Process modelling is widely used today for a variety of systems. Its main advantages are realised for systems which are complex and costly to analyse in other ways, such as a CHP plant [36]. For steady-state process modelling of a CHP plant, there are two general types of model simulations; design and off-design. Design simulations, carried out with nominal data, solves heat- and mass balances over the plant and further calculates the physical properties of the equipment units. These calculations are usually done for full plant capacity. In off-design simulations, the physical properties, such as heat transfer areas, are maintained from the design model [14, 27]. Input parameters such as plant load, ambient temperature and pressure, cooling water temperature and fuel quality are varied to study process outputs such as power and heat production [14, 27].

Seeing as CCGT plants should be able to operate at part load, it is of importance to be able to accurately describe the plant's part load behaviour [37]. This can be enabled with a process model, which further can be used for process optimisation purposes over a wide load range [24]. As a CCGT plant consists of several units, the process model can become complex since all units require an individual off-design model [37]. When describing the off-design behaviour of an HRSG, the objective is usually to predict the heat transfer coefficient of the heat exchangers [37]. Ganapathy [38] proposes a method which uses gas turbine off-design parameters, e.g. gas turbine exit temperature and mass flow, together with HRSG's thermodynamic design parameters to approximate the overall heat transfer coefficient [37, 38].

The gas turbine off-design performance can be estimated using several approaches. In highly accurate models, the gas turbine's components are treated separately. The compressor can be described according to a method suggested by Kim et al [37, 39], and the turbine's off-design performance can be predicted with the Stodola equation, Eq 4.1. This equation stems from an empirical correlation called Law of the Ellipse, developed by Professor Stodola [40].

$$\dot{m} = C_t \cdot \frac{p_{in}}{T_{in}} \sqrt{1 - \left(\frac{p_{in}}{p_{out}}\right)^2} \tag{4.1}$$

$p_{in}$ and $p_{out}$ represent the inlet and outlet pressures over the turbine stage, $T_{in}$ the inlet temperature and $C_t$ is the Stodola turbine constant [40]. Apart from describing a gas turbine, the Stodola equation is also applicable for steam turbines, where the mass flow of steam, $\dot{m}$, is the amount generated in the HRSG for CHP applications [37, 40]. The Stodola equation can, therefore, be used to correlate the turbine inlet mass flow to off-design conditions.

Off-design performance of a gas turbine unit can also be predicted utilising the nominal point of operation, usually provided by the manufacturer [24]. A simple, yet applicable model, which uses physical laws for describing and relating the off-design operation of a gas turbine to the nominal point, is presented below [24]. Starting with the ideal gas law, and rewriting it for mass flow, a relationship between the mass flows at design and off-design is obtained [24]. See Eq 4.2

$$\frac{\dot{m}}{\dot{m}_{design}} = \frac{pT_{design}A_c}{p_{design}TA_{c,design}} \tag{4.2}$$

where $p$ and $T$ are ambient pressure and temperature, $A_c$ crossectional flow area, and $\dot{m}$ the mass flow rate. From Eq 4.2, it can, for example, be seen that an increased ambient temperature decreases the mass flow in the gas turbine. Since the gas turbine power output is directly proportional to the mass flow, the power output decreases as the ambient temperature increases [24]. For geographical locations with varying outdoor temperatures, this parameter is of high importance. Note that applying this method involves several assumptions, such as a constant gas turbine efficiency, same deviations from ideal gas law at all loads, and a generator operated with constant speed [24].

## 4.2 Method - Model Development

The reference plant was modelled in the software EBSILON®Professional, which is a tool that can be used to simulate thermodynamic cycles such as CCGT-CHP plants [41]. The software enables simulation and design for retro-fitting and/or optimisation of plants using heat- and mass balances over components visualised in the program [41]. The purpose of the derived process model was to represent the reference plant, which was ensured by creating a design model based on operational data received from the plant owner.

The reference plant has three HRSG lines, but in order to analyse a wider set of operations, scenarios when only one or two lines are used are interesting to simulate. However, there are numerical challenges when having inputs of zero, thus variations of the original model were derived. The components used in these are exact copies of the original model, and behave in the same manner. Furthermore, to accurately describe the different operational strategies, off-design sub-models with and without supplementary firing as well as part load models were created. In total, six off-design models were derived from the design model, see Tab 4.2 in Section 4.3. In addition, the models with one or two HRSG line were designed with the

same off-design scenarios. Descriptions of the how the parts of the CCGT-CHP were modelled are presented in the following sections.

### 4.2.1 Gas Turbine

To model the gas turbines used in the reference plant, their characteristic curves at nominal and part load operating points were retrieved from the manufacturer. The specification correlates the ambient temperature and gas turbine load to a set of parameters, see Tab 4.1. The loads implemented in the model were chosen based on available information in the retrieved manufacturer data. In order to select appropriate ambient temperatures to incorporate in the model, the temperatures during plant operation were studied. Most operating hours occurred for ambient temperatures between -15 - 9 °C. However, to account for extreme values, a larger temperature interval, -15 - 20 °C, was incorporated in the gas turbine model.

**Table 4.1:** Parameters for gas turbine characteristics implemented in the process model. Note that the characteristic values without numbers are retrieved from manufacturer data.

| | **Parameter** | **Characteristic values** |
|---|---|---|
| Ambient temperature | $T_{amb}$ | -15, -5, 0, 5, 10 ,20 |
| Gas turbine loads | $L_{GT}$ | 100, 80, 60, 30 |
| Exhaust gas temperature | $T_{exhaust}$ | - |
| Exhaust mass flow | $\dot{m}_{exhaust}$ | - |
| Fuel mass flow | $\dot{m}_{fuel}$ | - |
| Water injection | $\dot{m}_{water}$ | - |
| Power generation | $P_{el}$ | - |

Data from the specification were implemented in a black box model, representing the gas turbine. The model utilises correlations between the parameters in Tab 4.1 and ambient temperature to create linear curves for different gas turbine loads. The reference plant's gas turbines have dry low emission operation, thus $\dot{m}_{water}$ was zero for all temperatures and loads in the gas turbine model.

When the model exhaust gas flow was compared to plant data, it was observed to be around 10 % lower. This underestimation lead to deviations in the succeeding model for HRSG and steam cycle. Therefore, the characteristic curves were increased by 10 % while maintaining the slope of the curves. A possible explanation for this deviation is that manufacturer specifications are valid for a new gas turbine, and thus not fully accurate for the gas turbines at the reference plant, which have been in operation for several years. This correction was only implemented for gas turbine loads above 60 %, since the part load operation did not show the same deviation.

For gas turbine load reduction, the reference plant reduces the fuel and ingested air flow. This operational strategy was implemented in the model characteristics

using manufacturer specifications at part loads. Furthermore, the reduced efficiencies occurring at part load operations were incorporated in the characteristic curves.

The fuel used in the model, and in the reference plant, was natural gas. According to plant data, its lower heating value should not be lower than 40 MJ/kg. The data from the gas turbine manufacturer was based on a heating value of 47 MJ/kg. Since the design of the gas turbine is mainly based on manufacturer data, a heating value of 47 MJ/kg was chosen as input for the fuel's heating value.

### 4.2.2 HRSG

The HRSG was modelled as shown in Fig 4.1. Based on the reference plant, it has a supplementary firing combustor (SF), three superheaters (SH1-SH3), one evaporator (EVAP), a feed water economiser (ECO) and a district heating economiser (DH ECO). The temperature after the first and second superheaters are set using live steam temperature controllers, see purple boxes in Fig 4.1.

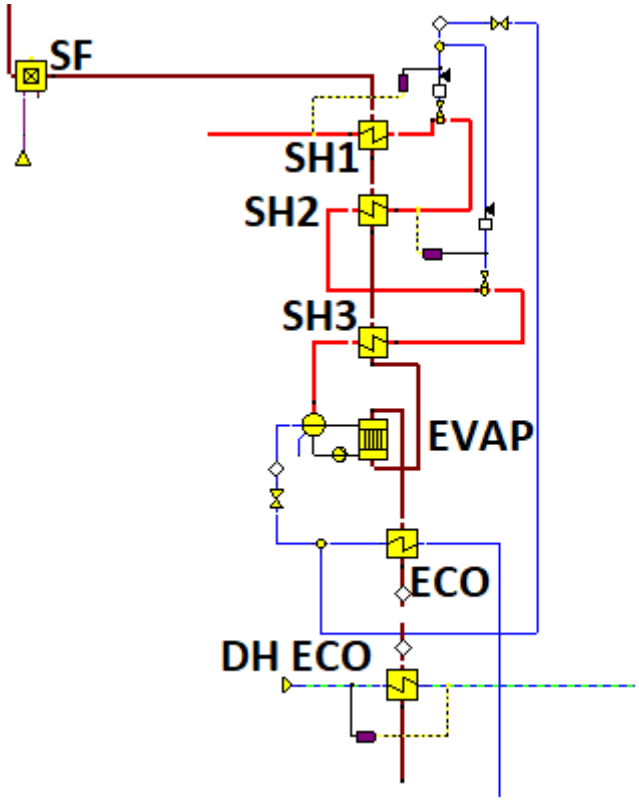


**Figure 4.1:** Illustration of the HRSG EBSILON®Professional model with a supplementary firing combustor (SF), three super heaters (SH1-SH3), one evaporator (EVAP), one feed water economiser (ECO) and a district heat economiser (DH ECO). The white squares are used in the model as input components, and do not correspond to process units.

The actual temperature of the exhaust gases after supplementary firing was not known due to lack of temperature measuring units at the reference plant. The

nominal temperature in the model was approximated to 940 °C based on energy balance including gas turbine load and fuel consumption for supplementary firing. The validity of this value was verified by a reference plant engineer. For off-design simulations, the amount of supplementary firing is entered as a boundary condition and regulated based on the desired heat and power output from the plant.

The superheaters are designed based on reference plant operating data. Their sizes were determined by the upper terminal temperature difference at nominal load, which is the temperature difference between incoming flue gases and outgoing steam. All steam temperatures were given in the operating data, but there was no temperature information for the flue gases. By modelling one superheater at a time, starting with SH1, the intermediate flue gas temperatures were obtained from energy balances over the component. From these, the upper terminal temperature differences could be calculated. From this design model, the sizes of the superheaters were determined and fixed for off-design simulations.

The attemperator system was designed using information on steam temperatures after feed water injection. The feed water flow in the design model was adjusted until the operating temperature of the steam and water mixture was obtained. For off-design calculations, a controller was used to control the water injection in order to ensure that the target temperature was not exceeded. The target temperature was different for the different plant load cases.

After the superheater section, the flue gases enter the evaporator, see Fig 4.1. In the model, the evaporator determines the mass flow in the steam cycle. From the mass flow, the pressure in the HRSG is determined, where a large mass flow correlates to a high pressure. At the steam turbine inlet, the steam is throttled to the corresponding swallowing capacity at the given mass flow. That is, the HRSG pressure is independent of the steam turbine, which utilises a valve throttling control strategy. The heat transfer area of the model's evaporator was approximated based on manufacturer drawings, see calculation approach in Appendix A. Furthermore, for off-design operation, the flue gas flow and temperatures are lower. To avoid pinch point violations, the evaporator temperature is decreased by reducing its pressure level. This is implemented in the model by having different evaporator pressures in the off-design models.

The flue gases' last heat exchange in the HRSG is the feed water economiser, which preheats high pressurised water. The exit water temperature from the economiser is modelled by inserting an approach temperature in the evaporator specifications. The approach temperature is the difference between saturation temperature and economiser outlet temperature.

The HRSG is equipped with a district heating economiser. In the reference plant, the district heating economiser consists of a closed water loop that heat exchanges with the flue gases, and then with a sub-stream of DHW. For modelling simplicity, the district heating economiser is resembled with a direct heat exchange with flue

gases and the DHW. This will, however, result in a larger heat exchange compared to the reference plant, why a higher stack temperature is used in the model as a correcting action. The model is equipped with a controller for the economiser. The aim of the controller is to manipulate the DHW mass flow in order to achieve a target temperature of the DHW, which varies depending on plant operation. Historical operating data revealed that the DH economiser load increased with a reduced plant and supplementary firing load. That is, the economiser does not fulfil its full load in the design case. To correct this, the heat transfer area was increased until the maximum load identified in the historical data was reached. Furthermore, having the flue gas stream directly entering the DH economiser in the model resulted in the economiser impacting the previous heat exchangers. To ensure that the DH economisers only uses the excess heat, and not affecting other units in the model, the flue gas stream was split after exiting the feed water economiser. The flue gas stream entering the DH economiser has the same thermodynamic state and mass flow as the one exiting the feed water economiser, which is ensured by setting a "input value" specifier accessing the values from the flue gas stream exiting the feed water economiser.

The heat exchangers' off-design performance in a CCGT-CHP is directly related to the heat transfer area and heat transfer coefficient. The nominal point of heat exchanger operation is related to the gas turbine's design point since the exhaust gases from the gas turbine determines the steam production. With this, and the corresponding design temperatures for the heat exchangers, the nominal point can be found. For off-design predictions, the product of the heat exchanger area and the heat transfer coefficient is kept constant, while other parameters such as temperatures and mass flows vary.

### 4.2.3 Steam Cycle

The steam cycle was modelled as shown in Fig 4.2. It consists of a control valve, two steam turbine (ST) stages with a generator, two condensers (C1 and C2) and a feed water tank (FWT). The district heat consumption is modelled as well as the extraction pressure control. The controller is the purple box in Fig 4.2.

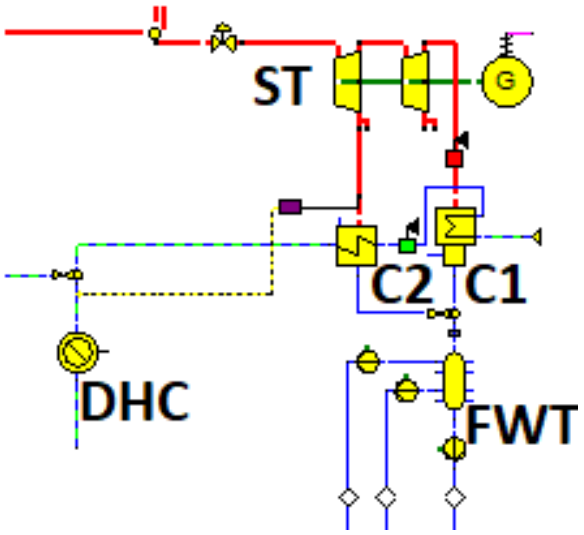


**Figure 4.2:** Modelled steam turbine (ST) and condensers (C1, C2) with a feed water tank (FWT) and a district heat consumption unit (DHC). The district heating water is the dashed green/blue streams, whereas the red is steam and the blue the cycle's water streams. The red, green and white squares are used in the model as input components, and do not correspond to process units.

After the steam streams from the different HRSG lines have been mixed, they enter the valve leading to the first turbine stage. The pressure after the valve is calculated in the first turbine unit according to the Stodola equation, Eq 4.1. As the mass flow of steam to the turbine is determined by the evaporators, and the outlet pressure by a controller, Stodola is solved for $p_{in}$, which alters the inlet turbine pressure depending on the mass flow of steam. This strategy corresponds to valve throttling pressure control, where the control valve opening is altered.

The steam turbine was modelled as two turbine sections; one for the extraction stage and one for the outlet. Due to lack of steam turbine specifications, the isentropic efficiency of each turbine unit was set to the software default of 88 %.

The extracted steam is condensed in a heat exchanger (C2) where it heats up the DHW. The extraction pressure, and thereby the temperature, was set by a controller to ensure that the exiting DHW reaches the supply temperature at both design and off-design operations. After condensation, the water is throttled down to the pressure of the first condenser (C1) before entering the feed water tank.

The remaining steam, which is not extracted, enters the second turbine unit. The design back-pressure was set to 0.5 bar according to process data. In off-design modelling, the back pressure was determined based on the temperature of the DHW entering C1. An upper terminal temperature difference of 4.33 °C between the steam and DHW was to be achieved, thus the back pressure varied to ensure the required steam temperature. Furthermore, in off-design, the temperature of the DHW after C1 was set to be half the required temperature lift over both condensers. After the condenser, the condensate enters the feed water tank, which is thereafter recycled

back to the HRSG.

The DHW from the last condenser (C2) is mixed with the DHW from the district heating economiser. Thereafter, the district heating load is modelled as a heat consumer, where the exiting temperature is set to that of the return DHW.

Furthermore, the reference plant has a direct condenser which enables steam turbine bypass. Instead of expanding the steam in the turbine, it is directly condensed to produce heat. In order to include this opportunity in the models, an additional off-design process model was derived. In this, the steam turbine in Fig 4.2 was replaced with a condenser. However, historical data for this scenario was not available, thus this model could not be validated nor adapted to actual operating conditions.

## 4.3 Results - Process Models

Six off-design models were created from the design model in order to represent the historical operation of the reference plant. A black box model approach was used where the model was adapted to operational process data, and details in unit behaviour were not considered. The derived off-design models are presented in Tab 4.2, with their characteristics and given model names.

**Table 4.2:** Derived off-design models with their applicable boundary conditions.

| **Off-design model** | **Model name** | **Gas turbine load [%]** | **Supplementary firing load [MW]** |
|---|---|---|---|
| 3 gas turbines<br>Full load with supplementary firing | A1 | >85 | >20 |
| 3 gas turbines<br>Full load without supplementary firing | A2 | >85 | <20 |
| 3 gas turbines<br>Part load | A3 | 30 - 60 | 0 |
| 2 gas turbines<br>Full load with supplementary firing | B1 | >85 | >20 |
| 2 gas turbines<br>Full load without supplementary firing | B2 | >85 | <20 |
| 2 gas turbines<br>Part load | B3 | 30 - 60 | 0 |

The need for several off-design models comes from the varying operating conditions at the different cases in Tab 4.2, which were chosen based on an analysis of historical plant data. For example, the live steam temperature and pressure are significantly higher in case A1 than A2. Thus, the developed process model consists of several off-design models and is therefore applicable for a wide range of operating conditions.

A figure of the full design model, Fig A.1, is included in Appendix A together with tables of inputs used and outputs analysed.

# 5
# Process Model Validation

To ensure that the derived process models represent the reference plant accurately, they were validated. This chapter starts with a theoretical background to model validation, followed by the method used in this study as well as the validation results.

## 5.1 Theory - Aspects of Validation

After a model has been constructed, its performance needs to be validated and analysed to see when it is applicable. The purpose of a validation is to compare the model estimations with real process data to ensure the accuracy of the model [42]. A process model validation should be designed in accordance with the context in which the process model exists [42]. Ideally, the model should re-generate the data set under the same circumstances at which the actual data is retrieved. For certain models, graphical and quantitative methods are sufficient whereas other require experimental methods using a pilot plant [42]. The validation process can be time- and resource consuming if it involves large amount of data and boundary conditions that are inserted in extensive models. Therefore, it is important to use a suitable validation method in order to maximise the benefits from each simulation [42].

A model's adequacy can be evaluated using residuals, i.e. the difference between the real value and model value, as in Eq 5.1 [43].

$$\varepsilon = y_{model} - y_{actual} \tag{5.1}$$

A residual analysis of an accurate model, which can be performed graphically, should not show evidence of clear residual patterns and can further give an indication of model inaccuracies [43]. From a residual analysis, biases can be identified which give rise to obvious pattern of errors. Furthermore, relative magnitudes of individual errors can be discovered [44]. One example is when extreme data points from the reference case cannot be obtained by the model, or when the model produces outliers [44]. The former mainly occurs due to failure in model derivation in which extreme points have not been considered [44]. Outliers should preferably be investigated further in order to improve model accuracy [43, 44].

## 5.2 Method - Validation of Process Models

The validation aimed at ensuring that the model produced results with the same trends as the reference plant data. The context of the validation is therefore mainly

trend identification, the model is not designed to exactly reproduce absolute values found in the reference plant data.

In the comparison, the off-design model that could best describe each operating hour was used, and the model was provided with the same inputs as the historical data point. Tab 5.1 shows the model inputs altered for each simulation run.

**Table 5.1:** Boundary conditions varied during process models' validation where the plant's outputs power and heat are compared.

| **Boundary conditions** |
|---|
| Gas turbine load |
| Ambient temperature |
| DHW supply temperature |
| DHW return temperature |
| Supplementary firing fuel input |

The validation aims at ensuring that the process models behaves as the reference plant does during the most reoccurring operational cases. These operations need to be identified from the historical data, which has an hourly time resolution, i.e 8760 data points. Furthermore, the data is non-cyclic, i.e. there is a significant, non-repetitive variation in the data set, and it is in a context where external factors influence the plant operation. Therefore, it is vital to sustain and include these characteristics when analysing and using the data [45]. In order to account for the characteristics in the reference plant data, parts from the method of characteristic operating pattern (CHOP) [45] were applied. In contrast to sort the data in chronological order, this method allows sorting on other parameters. The data set is reduced to a number of scenarios containing similar operating points while sustaining the characteristics of plant operation [45]. For example, data points where all three gas turbines were turned-off has been removed from the data set. Gas turbine load, as well as ambient temperature and supplementary firing loads, have been used as sorting parameters for the remaining data set as they highly influence the plant performance. Scenarios of different combinations of these parameters have been formulated to simplify the validation. Furthermore, the operating hours analysed were all steady-state points at which the plant had operated at the current capacity for at least 4 hours. That is, transient data points were not considered.

One of the two quantitative validation measures used was analysis of the percentage conformity, $\gamma$, as in Eq 5.2, which was calculated by dividing the historical power or heat output with corresponding model output.

$$\gamma = \frac{y_{actual}}{y_{model}} \tag{5.2}$$

Additionally, a residual analysis was performed according to Eq 5.1.

By studying the temperature profiles for the temperatures, in Tab 5.1, strong correlations were observed. When the ambient temperature increased, the supply and

return temperature of the DHW decreased accordingly. Therefore, it was considered enough to include only one of these parameters when performing the residual analysis. The significant impact of ambient temperature on gas turbine power output, see Eq 4.2, together with the varying climate in Gothenburg, ambient temperature was chosen as the temperature boundary condition to include.

## 5.3 Results - Process Models' Validity

During the validation of the process models, it was identified that the plant's power output was constantly overpredicted by approximately 10 MW. The overprediction can be due to several reasons. Firstly, the model represents a new plant, without degradation and aged equipment, which hardly is the case in the reference plant which has been in operation for several years. If the reference plant has had the same annual full load hours from plant start-up until 2016, the plant output is approximately reduced by 7 % only due to gas turbine ageing and degradation, according to the discussion in Section 3.1.1. Secondly, the measuring point of power output in the reference plant data is unknown. Whether the measured power is shaft power, generator power, or grid power can contribute to a deviation in simulation results. Due to the overprediction, the complete model consists of the one created in the simulation software with the addition of subtracting 10 MW from its power production.

In Fig 5.1, the heat and power outputs from models with three gas turbines, A1-A3, are graphically compared to historical data points with the same operating conditions. The black x-axes in the figures indicate the ambient temperature for the overlying data points, which are not in chronological order but sorted based on ambient temperature. The temperatures used in each model validation are based on availability of historical data. Note that the figures do not contain all data points used in the validation procedure. The corresponding validation figures for operation with two gas turbines, B1-B3, are presented in Appendix B.

**(a)**

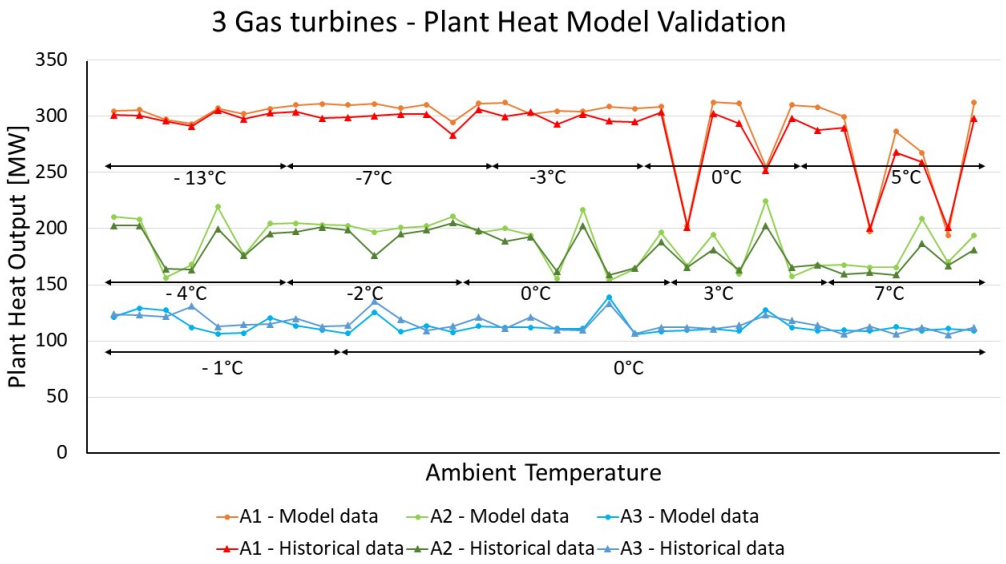


**(b)**

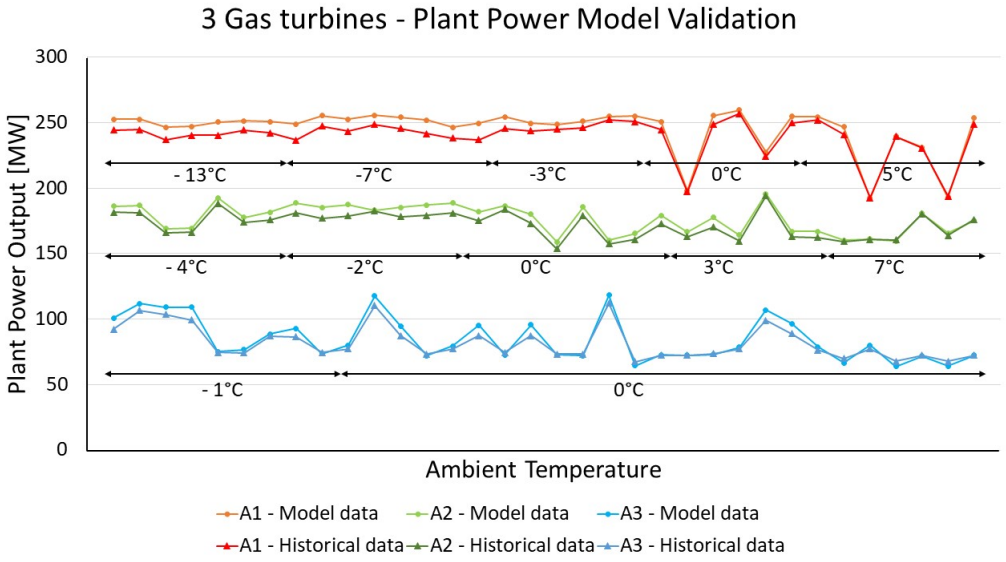


**Figure 5.1:** Three off-design models' a) heat and b) power output compared to historical data for the same operating conditions. Data points sorted based on ambient temperature, as shown by the black lines. Model names according to Tab 4.2.

From Fig 5.1, the models were considered to reproduce the trends in the historical data in a satisfactory manner for both heat and power. Furthermore, as the model and historical data lines often overlap, the model values are generally similar to the historical ones. This is further analysed in the residual analyses graphically shown in Fig 5.2 for models A1-A3. The residual analyses for models B1-B3 are included in Appendix B.

**(a)**

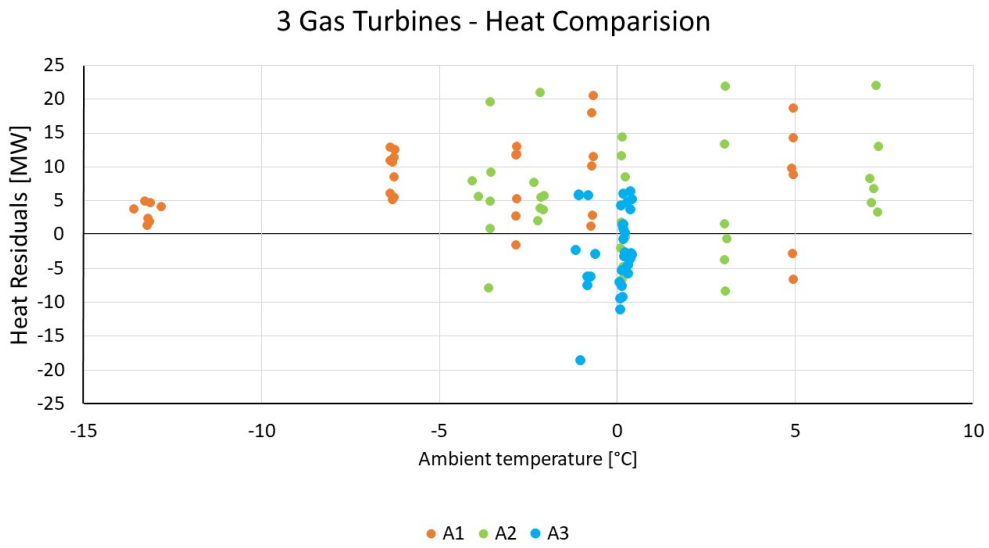


**(b)**

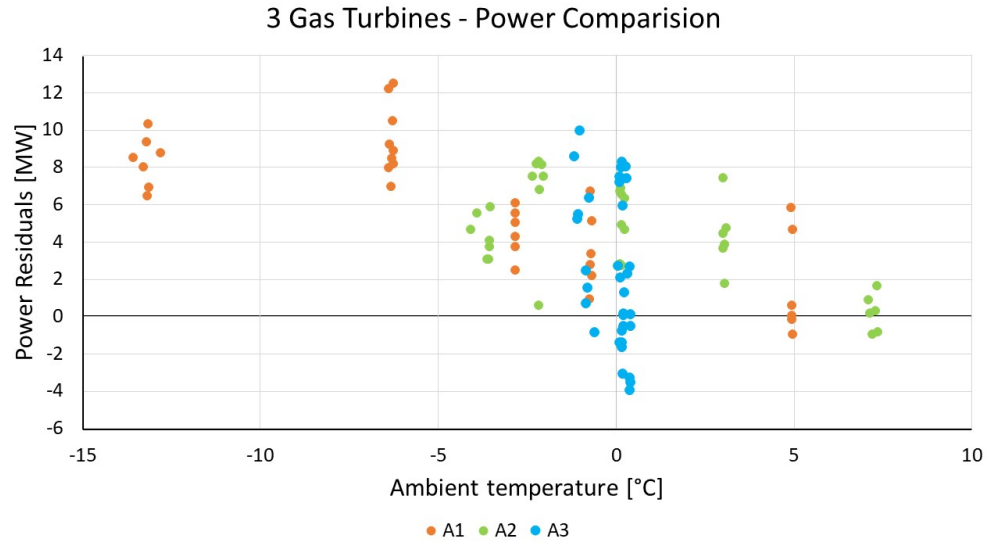


**Figure 5.2:** Graph for three off-design models' a) heat and b) power output residuals with different y-axis scales. Model names according Tab 4.2.

From Fig 5.2 a), it can be seen that there is a difference in the residual analyses for the three process models, A1-A3. The validation of each model has been performed for available ambient temperature for each operating setup, why only A1 has been validated for temperatures below −5 °C. Furthermore, the heat residuals for A1 show a widening trend where the model mainly overpredicts the heat output. This is likely a result from the DHW economisers, which were more accurate at low temperatures. However, seeing as A1 represents full plant capacity, the size of the residuals is not alarming as the percentage conformity is not linear to the magnitude of the deviation. In contrast, neither A2 nor A3 have a clear residual trend. Furthermore, they are most accurate around their design ambient temperature 0-4 °C.

In contrast to the heat output, where the model both under- and overestimated, the plant power output is mainly overpredicted, see Fig 5.2 b). Note, however, the different y-axis scales in Fig a) and b), which is smaller for b). As for heat, A1 is the model with the largest deviation in power output, where the deviation decreases with an increased ambient temperature. Ambient temperature highly influences the power output from the gas turbines, where low temperatures are correlated to an increased output. This correlation might be stronger in the model than in the historical data, why also the power output for A2 and A3 are mainly overpredicted by the model.

As the context of the validation was trend conformity, which was considered satisfactory, the deviations shown in the residual analyses were considered acceptable. In Tab 5.2, the average as well as maximum over- and underpredictions are presented for power and heat for the six off-design models. The table shows that the average deviations for both heat and power were below 5 % for all models, which was considered a tolerable deviation.

**Table 5.2:** Percentage conformity from historical data for power and heat output for six off-design models.

| **Off-design model** | **Power** | | | **Heat** | | |
|---|---|---|---|---|---|---|
| | **Average deviation** [%] | **Max. under-estimation** [%] | **Max. over-estimation** [%] | **Average deviation** [%] | **Max. under-estimation** [%] | **Max. over-estimation** [%] |
| A1 | 2.67 | 0.5 | 6.9 | 2.3 | 3.4 | 6.8 |
| A2 | 2.39 | 0.91 | 5.2 | 2.5 | 7.3 | 11.8 |
| A3 | 2.1 | 6.2 | 9.1 | 2.1 | 20.2 | 8.8 |
| B1 | 1.6 | 1.9 | 4.0 | 3.6 | 1.3 | 8.6 |
| B2 | 0.2 | 3.1 | 5.0 | 4.5 | 5.3 | 12.8 |
| B3 | 0.8 | 4.3 | 6.9 | 2.2 | 5.8 | 5.7 |

Furthermore, Tab 5.2 shows that A3 has the largest heat and power overpredictions. However, these outliers did not affect the average deviation significantly as A3 has the lowest average deviation for heat calculations. Therefore, this outlier was not corrected.

Overall, the validation showed that the models could predict the plant performance in a adequate way for the ambient temperature intervals analysed.

# 6
# Process Model Linearisation

To find optimal operating strategies for the reference CCGT-CHP plant, the process models were linearised to a set of equations which mathematically describe the plant. The formulated equations were then used in an optimisation model through which optimal operating strategies are identified. This chapter starts with a theoretical background to linearisation, followed by the method used in this project. Finally, the resulting linear equations are presented and discussed.

## 6.1 Theory - Linearisation

Linearisation is a statistical tool to predict the behaviour of a non-linear system in an operating region [43, 46]. It is used to describe the relationship between variables and the resulting response with a mathematical equation [46]. A linearisation can consist of two main parts where the first is to identify important parameters and their extreme values and, secondly, to set up a mathematical formulation of the studied system.

In systems where there are several factors affecting the output, factorial design is useful [43, Ch.5]. The purpose of factorial design is to capture how the different factors influence the system response [43, Ch.5]. This is done by including all combinations of factors at every factor level while studying how the response variable change [43, Ch.5]. A common factorial design is the $2^k$ method [43, Ch.6]. This consists of two qualitative levels for each of the k quantitative factors [43, Ch.6]. The levels are often chosen as high and low, and the factors can be any quantitative measure such as temperature, pressure, or power [43, Ch.6]. To perform a $2^k$ factorial design, $2^k$ observations are required [43, Ch.6].

For a response variable, $y$, which is related to $k$ regressor variables, $x_1$, $x_2$,...,$x_k$, a general mathematical formulation for a linear regression model can be formulated as in Eq 6.1 [43, Ch.10].

$$y = \beta_0 + \beta_1 x_1 + \beta_2 x_2 + ... + \beta_k x_k + \varepsilon \tag{6.1}$$

The parameters $\beta_i$ are regressor coefficients that represent the change in response per unit of change in the corresponding factor, $x_i$, and $\varepsilon$ is an error term [43, Ch.10]. This formulation creates an operating region of k-dimensions with $\beta_0$ as the plane interception with the response axis [43, Ch.10]. In some systems, the interaction between parameters is vital to include to accurately describe the system. In these cases, an interaction term, $x_i x_j$, is included in Eq 6.1 [43, Ch.6].

In a $2^2$ factorial design, values for $\beta_i$ are estimated by assigning $x_1$ and $x_2$ with levels of low (-) and high (+). These are combined and altered one at a time in order to receive information of the combination of the variables, see Tab 6.1 [43, Ch.6].

**Table 6.1:** Combinations of factor levels in a $2^k$ factorial design.

| $\mathbf{x}_1$ | $\mathbf{x}_2$ |
|---|---|
| - | - |
| + | + |
| + | - |
| - | + |

The parameters, $\beta_i$, are found using linear regression methods, where the factors are correlated to the experimental responses found using an experimental setup as in Tab 6.1 [43, Ch.5]. They can be estimated using a least square method, which aims to find values of the coefficient that minimise the error [43, Ch.10]. The error is the observed value subtracted by the model response prediction, i.e. the residual [43, Ch.10]. Once values for $\beta_i$ have been found, an operating region is formulated in which points between the extreme values can be found via linear interpolation [43, Ch.5].

To obtain information about the regression model's performance, the $R^2$-value can be studied. This is a measure of how well the response's variability is predicted by the model and its regressor parameters [43, Ch.10]. The $R^2$-value is between 0 and 1, where 1 indicate low variability, why a value close to 1 is preferable [43, Ch.10].

## 6.2 Method - Linearisation of Process Models

The factors included in the linearisation of the process models were selected as the boundary conditions used in process model validation, see Tab 5.1, as they highly influence the plant performance. Linearised equations of how these factors affect the plant's power and heat production, as well as fuel consumption, were created using the linear regression method with factorial design. In this setup, all interaction parameters are neglected. The off-design process models were run for all factor combinations to obtain response values for power, heat, and fuel consumption. Using the response for every combination of design factor levels, the parameters, $\beta_i$, in the linear regression equations were found using the least square method.

Performing a factorial design and linear regression of the factors presented in Tab 6.2, with three gas turbines and three supplementary firing units, implied the need for $2^9$ observations corresponding to 9 design factors and 10 parameters. To reduce the complexity of the linearisation, the gas turbines were viewed as one unit, as were the supplementary firing combustors. Thereby, the factorial design was reduced to a $2^5$ factorial design with 32 combinations rather than the 512 required for a $2^9$ fac-

torial design. The selected parameters to linearise are presented in Tab 6.2 together with their + and − values, which were identified from historical data.

**Table 6.2:** Identified low (−) and high (+) levels for CHP design factors. Note that the gas turbine system load refers to the total load of all three gas turbines.

| **Factor** | **Unit** | **Symbol** | − | + |
|---|---|---|---|---|
| Gas turbine system load | - | $L_{GT}$ | 0.1 | 1 |
| DHW supply temperature | $[K]$ | $T_{DH,s}$ | 340 | 380 |
| DHW return temperature | $[K]$ | $T_{DH,r}$ | 310 | 325 |
| Plant supplementary firing input | $[MW]$ | $Q_{SF}$ | 0 | 237 (79) |
| Ambient temperature | $[K]$ | $T_{amb}$ | 258 | 293 |

The gas turbine characteristics from the manufacturer were available at loads between 30-100 %, as this is the operating region for them. This implies that the formulated model is not applicable for individual gas turbine loads below 30 %. Having only one gas turbine at 30 % sets the (−) value for the combined gas turbine system to 10 %, as in Tab 6.2.

The (+) value for the supplementary firing system is the largest amount of supplementary firing used for one combustor at the reference plant multiplied with three. This was done in order to represent the whole supplementary firing system. However, running the process model at the (−) value for gas turbine load, and (+) value for supplementary firing load, implied having a fuel input to one combustor at three times its capacity. Therefore, for the combinations with (−) value for gas turbine load, the (+) value for supplementary firing load was chosen as the highest value for one supplementary firing combustor. That is, 79 MW.

In the CHP plant, power can be produced from both the gas and steam turbines. The factors influencing the power production in the steam turbine are as in Tab 6.2, whereas the factors affecting the gas turbine power are only ambient temperature and gas turbine load. To account for these different factor combination, one equation was formulated for the gas turbine system, and one power equation for the steam turbine, where the plant power output is the sum of these two, see Eq 6.2.

$$P_{plant} = P_{GT} + P_{ST} \tag{6.2}$$

Furthermore, fuel is added to the system either in the gas turbine or as supplementary firing. The gas turbine fuel consumption was linearised with gas turbine power output as its only factor. The factor for supplementary firing is the amount of fuel added multiplied with the fuel's lower heating value, thus $Q_{SF}$ is already correlated to fuel input. The plant's fuel consumption is therefore the sum of the linearised equation for gas turbine fuel and the supplementary firing value.

The reference plant has the alternative to fully bypass the steam turbine and condense the steam directly to heat exchange with the DHW. The heat output when

utilising the steam turbine or the direct condenser differs significantly, hence, two linear heat equations are necessary; one for full bypass and one representing heat output during steam turbine utilisation. However, both heat equations' factors are as in Tab 6.2. For scenarios with full bypass, the gas turbine is the only power producing unit.

After linearising the process model, the equations were validated against process models' output. The calculated values and the output from the process model for the extreme values in Tab 6.2 correlated well, the $R^2$-values were all above 0.98. The equations were further validated against process model output at operating conditions found in the reference plant data from 2016. During the validation, it was observed that the heat equation for steam turbine utilisation and steam turbine power deviated the most from process model values. By adding values for operating hours utilising the steam turbine to the factorial design, both equations performed satisfactory for all process models A1-B3. The results from the validation procedure are included in Appendix C.

## 6.3 Result - Linearised Model

The linearised equations are all a version of Eq 6.3

$$y = \beta_0 + \beta_{L_{GT}} L_{GT} + \beta_{T_{DHW,s}} T_{DHW,s} + \beta_{T_{DHW,r}} T_{DHW,r} + \beta_{Q_{SF}} Q_{SF} + \beta_{T_{amb}} T_{amb} \quad (6.3)$$

where $y$ is either gas turbine power, steam turbine power or heat with or without steam turbine bypass. Each factor's corrected parameters, $\beta_i$, in the linearised equations are presented in Tab 6.3.

**Table 6.3:** Parameter-values for power and heat responses.

| **Parameter** / **Response** | $\beta_0$ | $\beta_{L_{GT}}$ | $\beta_{T_{amb}}$ | $\beta_{T_{DH,s}}$ | $\beta_{T_{DH,r}}$ | $\beta_{Q_{SF}}$ |
|---|---|---|---|---|---|---|
| $P_{GT}$ | 82.99 | 137.69 | -0.30 | - | - | - |
| $P_{ST}$ | 102.85 | 39.74 | -0.04 | -0.07 | -0.19 | 0.36 |
| $Q_{nobypass}$ | 134.55 | 147.60 | -0.16 | 0.03 | -0.18 | 0.56 |
| $Q_{fullbypass}$ | 222.52 | 199.11 | -0.14 | 0.20 | -0.63 | 1.03 |

As seen in Tab 6.3, $\beta_{T_{amb}}$ is negative in all equations. This is a result from the ambient temperature's influence on the gas turbine performance. An increased ambient temperature decreases the power output from the gas turbine as well as the exhaust gas flow. Consequently, there is less heat available for the HRSG and, therefore, less steam available for heat and power generation in succeeding units.

In Tab 6.3, values for $\beta_{T_{DH,s}}$ are positive for both heat equations but negative for $P_{ST}$. Seeing as an increased supply temperature results in an increment of the extraction pressure in C2, the power generation is reduced and, hence, $\beta_{T_{DH,s}}$ for $P_{ST}$ is negative. When comparing the heat equations, it can be seen that $\beta_{T_{DH,s}}$ is smaller

for $Q_{nobypass}$ than $Q_{fullbypass}$. This might be a result from the different condensers used. When operating with the steam turbine, the DHW is heated in two steps, where the first condenser, C1, is not as affected by the $T_{DH,s}$ whereas the second one, C2, is. In contrast, when operating with full bypass, only one condenser is used, which is more affected by the $T_{DH,s}$ than the combination of C1 and C2 is.

The negative value of $\beta_{T_{DH,r}}$ for the $P_{ST}$ response in Tab 6.3 comes from the increased back pressure in C1 when the return temperature increases. An increased back pressure results in a smaller power production in the steam turbine. Furthermore, it also limits the heat production as the heat of condensation reduces with an increased pressure, thus the parameter values are negative for $Q_{fullbypass}$ and $Q_{nobypass}$ as well.

Tab 6.3 further shows a positive value of $\beta_{Q_{SF}}$ for all responses, where the one for $Q_{fullbypass}$ is larger than for $Q_{nobypass}$ and $P_{ST}$. This is due to that all supplementary firing energy is fully allocated for heat production when bypassing the steam turbine, whereas for the other case, the energy is divided between power and heat. The same reasoning applies for $\beta_{L_{GT}}$, which is the highest for $Q_{fullbypass}$.

Furthermore, the equation for plant fuel consumption was formulated according to Eq 6.4.

$$Q_{fuel} = 31.05 + 1.90P_{GT} + Q_{SF} \tag{6.4}$$

In conclusion, the linearisation of the process model consists of five equations; four versions of Eq 6.3 describing the responses in Tab 6.3, and a fuel equation as in Eq 6.4.

# 7
# Process Operation Optimisation

The final step in this work was to create an optimisation model which identifies profitable operating strategies for the reference CCGT-CHP plant. The optimisation model's foundation is the linear equations of the process models. The mathematical optimisation model therefore utilises the outputs from previous steps in this project, and combines them to answer the case study questions. This chapter describes the method used to create an optimisation model as well as descriptions of possible future energy scenarios.

## 7.1 Method - Optimisation Model Development

With the aim to find strategical operating conditions of the CHP plant, the optimisation tool GAMS was used. It is based on mathematical algebra and the concept of programming [47]. The programming language consists of four elements; sets, parameters, variables, and equations, where the latter should be functions of parameters and variables.

The equations derived with linear regression were implemented in the optimisation software together with sets, parameters, and constraints to be fulfilled during calculations. The main objective of the optimisation was to maximise plant revenue. This was calculated for each operating hour, $t$, according to Eq 7.1

$$r(t) = P_{el}(t)C_{el}(t) + Q_{DH,demand}(t)C_{DH}(t) - Q_{fuel}(t)C_{fuel} \tag{7.1}$$

where $r$ is revenue, $P_{el}$ the plant's total power production calculated according to Eq 6.2, $C_{el}$ is the electricity price, $Q_{DH}$ produced heat, $C_{DH}$ district heating price, $Q_{fuel}$ fuel consumption and $C_{fuel}$ is the fuel price.

The price for district heat was inserted in the model as an input file, which had a seasonal fluctuation with higher prices during colder periods. In addition, hourly electricity prices were provided to the model, as well as a constant natural gas price of 333.5 SEK/MWh [1]. All inputs and outputs, together with optimisation variables and constraints used in the model are presented in Tab 7.1.

**Table 7.1:** Inputs, optimisation variables and constraints provided to the optimisation model as well as model outputs.

| **Parameter inputs** | **Optimisation variables** | **Outputs** | **Constraints** |
|---|---|---|---|
| Ambient temperature | Gas turbine load | Heat production | $0.1 \leq L_{GT}(t) \leq 1$ |
| DHW return temperature | Supplementary firing | Gas turbine power | $Q_{SF}(t) \leq Q_{SF,max} L_{GT}(t)$ |
| DHW supply temperature | | Steam turbine power | $\mathrm{Q(t)} \geq Q_d(t)$ |
| Electricity price | | Fuel consumption | |
| District heating price | | Revenue | |
| Fuel price | | | |
| Heat demand | | | |

Additionally to the price inputs, hourly heat demand and ambient temperature were used as model inputs, see Tab 7.1. Ambient temperature was the temperature measured during 2016, and heat demand the produced heat at the reference plant during each operating hour of 2016. That is, it was assumed that the heat demand would remain the same as during 2016 and therefore used as a constraint that the optimised operation needed to fulfil. Furthermore, it was assumed that only the demanded heat could be sold, thus this amount was included in the objective revenue function, Eq 7.1. However, the model was allowed to produce more than the demand if this was profitable, and the surplus heat was assumed to be cooled off in a nearby river.

The optimisation variables in Tab 7.1 were calculated by the linearised equations in a way that ensured a maximised revenue for each hour studied while fulfilling all constraints.

In order to use linear programming, and have the possibility to utilise steam turbine bypass, two optimisation models were required; one representing full steam turbine bypass and one with no bypass possibility. The difference in the two models were the equations used for heat. For the full bypass alternative, $Q_{fullbypass}$ and $P_{GT}$ in Tab 6.3 were used for heat and power generation calculations, respectively. Consequently, $Q_{nobypass}$, $P_{ST}(t)$ and $P_{GT}$ in Tab 6.3 were applied for the no bypass option. That is, for full bypass, the plant's power is generated from the gas turbines, whereas for no bypass, power is produced from both the gas turbines and steam turbine as in Eq 6.2. Furthermore, linear programming does not allow multiplication of variables with other variables. Otherwise, multiplication with binary variables could have been used to switch between equations, but sine this was not possible, the need for two models arose.

The gas turbine load can only obtain values between 0.1 and 1, which was implemented as a constraint in the optimisation model according to Tab 7.1. This implies that the model cannot provide values for gas turbine loads of zero, nor above its maximal capacity.

For full gas turbine loads, the oxygen content in the exhaust gases is sufficient for supplementary firing combustion. However, for part gas turbine loads, the oxygen availability can be limited, which sets a restriction of supplementary firing utilisation at these loads. This constraint was incorporated in the optimisation model in accordance with Tab 7.1. By studying the exhaust flow from the gas turbine, it was observed that the reduction of oxygen concentration was relatively proportional to the corresponding load decrement. That is, a 10 % load reduction was rather equivalent to a 10 % decrement in oxygen concentration. This finding was used to formulate the constraint in Tab 7.1, which relates each operating hour's maximum supplementary firing load to gas turbine load. Note that $Q_{SF,max}$ is the (+) value found in Tab 6.2.

With the parameters in Tab 7.1, together with the constraints presented, the optimisation models maximise the revenue at each operating hour using linear programming. Thus, at each operating hour, the optimisation models find the loads for the gas turbine system, as well as for the supplementary firing system, that results in the highest revenue for the input data presented in Tab 7.1. For each simulation, both optimisation models are run individually. Post-treatment of the output data from the optimisation models were performed to select the model that obtained the largest revenue. That is, if the bypass model achieved the largest revenue, its variables' values were selected for the studied operating hour for further analyses. The resulting data analysed was therefore a combination of the results from the two optimisation models.

The models were run for the reference plant's values during 2016 in order to compare the operational strategies with the ones used. In addition, the optimisation models were run for different possible future energy market scenarios, as well as used for sensitivity analyses to evaluate the plant's revenue in different scenarios.

### 7.1.1 Scenarios and Sensitivity Analysis

Scenarios were studied to analyse the CHP plant's profitability in possible future energy systems. The additional scenarios studied are based on an energy system with an increased wind power penetration, see Tab 7.2. The scenarios, suggested by Romanchenko et al. [8], are based on projected future wind profiles for 2030.

**Table 7.2:** Analysed scenarios' wind power penetration [8, 48].

| **Scenario** | **Wind power penetration** [TWh] | % **of electricity from wind** |
|---|---|---|
| Reference, 2016 | 15 TWh | 9% |
| S1 | 15 TWh | 10 % |
| S2 | 26 TWh | 20 % |
| S3 | 50 TWh | 35 % |
| S4 | 70 TWh | 50 % |
| S5 | 70 TWh, No nuclear | 50 % |

Scenarios S1-S4 have different penetration of wind power, while sustaining the electricity generation mix of 2012 [8]. That is, the wind power production increases from S1-S4. In contrast, scenario S5 assumes a different electricity generation mix as it represents the case of a total phase out of nuclear power [8].

The scenarios have different electricity prices since it is the marginal cost that is used to determine the electricity price for each hour, and this cost depends on the amount of available wind power [8]. That is, the merit-order changes for the different scenarios and, subsequently, affects the market electricity prices. Furthermore, since the operating cost for wind power is relatively low, the electricity prices will also fluctuate more frequently with an increased wind power penetration. Note that the electricity price in the reference case (2016) and for the scenarios are for the price area of Gothenburg, Sweden [8].

In addition, a sensitivity analysis was performed for natural gas price, which was based on the taxation of fossil fuels and $CO_2$-taxes. Depending on a country's legislation and current political strategies, future $CO_2$-taxes are hard to predict [49]. However, future taxation scenarios for Sweden have been made by Naturvårdsverket [49]. These generally consist of two taxation strategies for power plants covered by EU's emission trading system (EU-ETS); full energy taxation, or full energy- and $CO_2$ taxation. For these two scenarios, the natural gas price, including taxes, is expected to increase to 469 or 672 SEK/MWh, respectively [49].

Furthermore, the profitability and possibility of implementation of a thermal storage tank was examined. By adding an additional constraint to the model, which allowed the produced heat to be 10 % less than the heat demand, the amount of excess heat produced was compared to deficiency hours. The amount of under-production was compared to the amount of surplus heat to see if these could even out.

# 8

# Project Results and Discussion

## 8.1 Profitable Operational Strategies

The optimisation model which resembled the reference plant's operation the most was the one always utilising the steam turbine, "No Bypass". In Fig 8.1, comparisons are made between this one and historical data for gas turbine power output and the use of supplementary firing respectively.

**(a)**

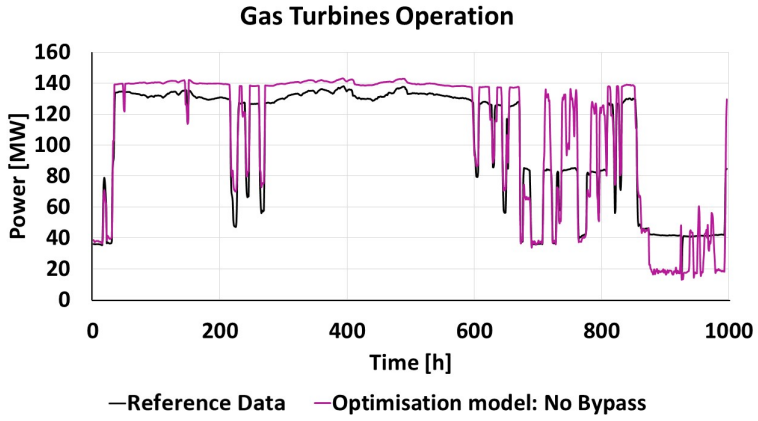


**(b)**

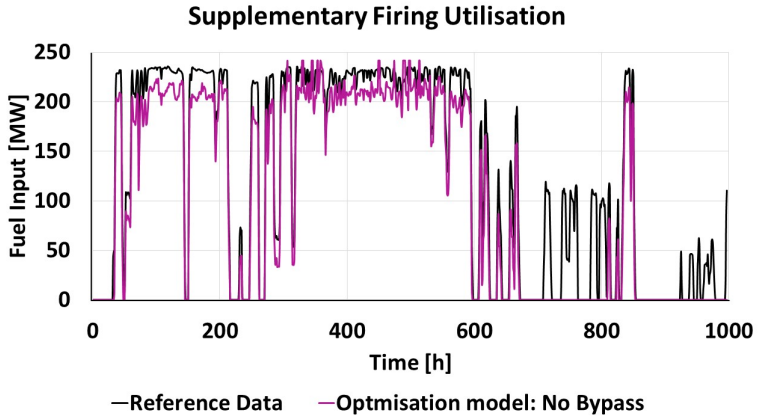


**Figure 8.1:** Comparison between reference plant operations and the optimisation model for steam turbine utilisation. Fig a) represents the gas turbine power output and b) the supplementary firing utilisation.

The optimisation model for no steam turbine bypass ("No bypass") showed a similar way of utilising supplementary firing as the reference plant data; it is mainly used

when all gas turbines are operated at full load. However, in Fig 8.1, there are some operating hours, 800-1000, where the reference plant utilised supplementary firing without being at full plant capacity. Throughout the year, it was only a small share of operating hours using this strategy. When comparing the reference data with data from the optimisation model for these hours, it can be seen that the model chooses to fluctuate the gas turbine load, whereas the reference data shows a fluctuating pattern for supplementary firing. That is, it seems as both vary the plant output to profit from high electricity prices. To fluctuate the supplementary firing, as the reference plant, might be preferable from an operating point of view rather than varying gas turbine load.

Furthermore, the graph in Fig 8.1 a) shows that the maximum gas turbine output is larger for the optimisation results than the reference data. This is likely a result from the overpredicting process model and follows the results in the validation of this. Overall, the figures show a strong resemblance between gas turbine power output and supplementary firing utilisation. From this, it seems as the calculated values are reasonable and that the reference plant has been operated in a rather revenue maximised manner.

For utilisation of the direct condenser ("Full Bypass"), however, the optimisation model chose to use supplementary firing even if the gas turbines operated at part loads. According to the optimisation model, operation of the direct condenser was the most profitable strategy during hours with low electricity prices. That is, it was more profitable to allocate the input fuel to heat production rather than producing power in the turbines, which would require more fuel to fulfil the heat demand. For full bypass operation, the power-to-heat ratio, $\alpha$, was decreased compared to the reference plant's operations.

The scenarios in Tab 7.2 were simulated in the optimisation model. By analysing the optimised operations for them, it was identified that utilisation of the direct condenser increased for scenarios with larger wind power penetration. See Fig 8.2, which shows the percentage of operating hours bypassing the steam turbine compared to those with no bypassing.

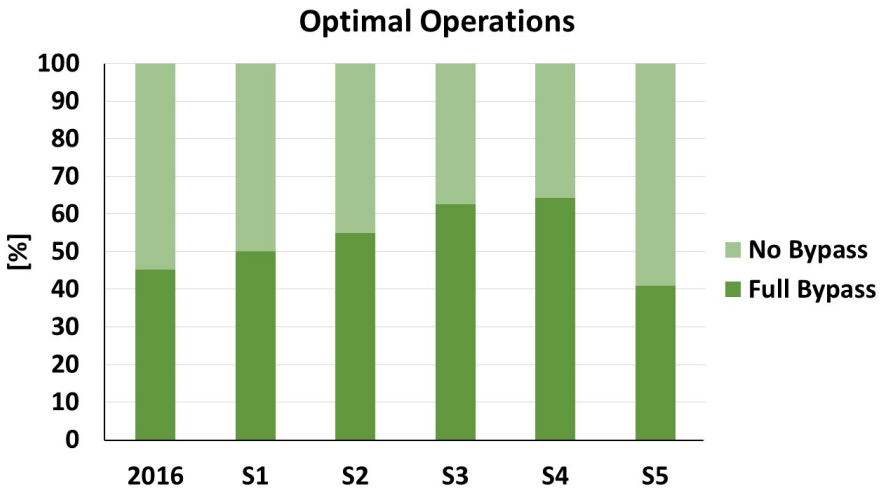


**Figure 8.2:** Share of operating hours with and without steam turbine bypass for scenarios in Tab 7.2 during optimal operations.

Due to the increased penetration of wind power in the system, and the constant electricity mix, the average electricity price is lower for scenarios S1-S4 compared to 2016. Consequently, an increased share of operating hours utilising full bypass is found for these scenarios, see Fig 8.2. The overall decreased electricity prices in S1-S4 generally decreases the profitability of the CHP plant. However, the heat demand needs to be fulfilled, which is most profitably achieved via the direct condenser. In contrast, scenario S5 has the smallest share of operating hours utilising the direct condenser. This is most likely a result from the changed electricity mix, where capacity has been removed from the system. As the cheap electricity production of nuclear power is no longer available, the average electricity price is increased and, therefore, it is more profitable to produce power in the steam turbine. In conclusion, penetration of cheap power producing sources increases the need for direct condensing opportunities in order to have the most profitable operation. However, a changed electricity mix, like S5, might eliminate the linear relationship between wind power penetration and power-to-heat ratio.

To analyse the implications of switching between steam turbine and direct condenser, the graphs in Fig 8.3 were derived. In Fig 8.3 a), the total yearly revenue is plotted for the different scenarios when operating according to Fig 8.2, "Optimal", or when no steam turbine bypass is allowed, "No bypass". The numbers were obtained by summarising the revenue for each operating hour. In Fig 8.3 b), the total annual power production for each scenario is presented. Finally, the chart in Fig 8.3 c) shows the number of operating hours the gas turbine load has changed with more than 20 percent points from one hour to the next. This was derived in order to analyse fluctuations in gas turbine operations.

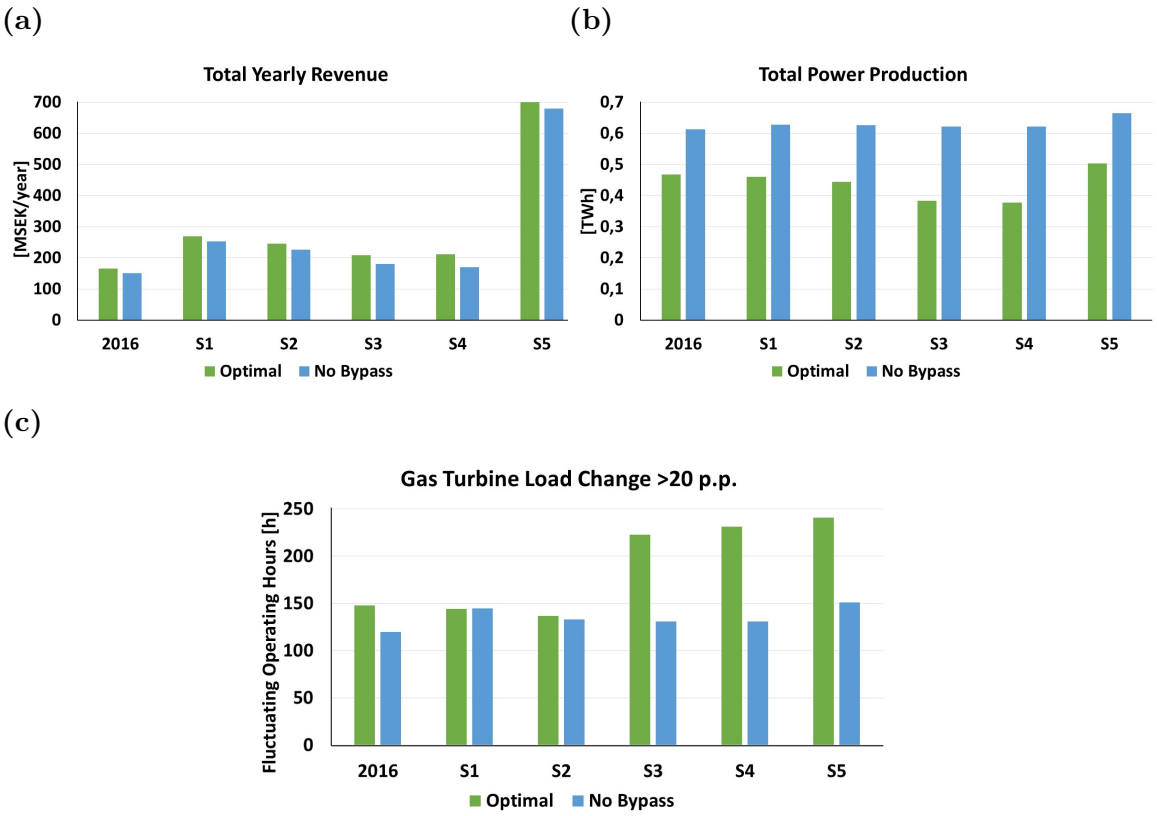


**Figure 8.3:** Suggested operating conditions, for scenarios in Tab 7.2, conducted for an optimal mix of steam turbine and direct condenser which is compared to operations with only the steam turbine. The variables compared are a) total yearly revenue, b) total power production and c) the fluctuations in gas turbine load.

For scenarios S1-S4, the total yearly revenue is decreased as the wind power penetrations increases, see Fig 8.3 a), which is likely a result of the decreased average electricity price. From the figure, it can be seen that S5 is the most profitable scenario, which might stem from its large average electricity price. From Fig 8.3 a), it does not seem to be a remarkable difference in revenue between optimal operations and "No bypass". Nevertheless, the optimal operations had a 24 % higher yearly revenue for S4. This is the scenario with the largest share of direct condenser utilisation, see Fig 8.2, thus the difference between the two cases is the largest. Even though the optimised operations utilised direct condensation during at least 40 % of the analysed hours (see Fig 8.2), the yearly revenue shows profitable operations for utilising the steam turbine for all operating hours.

The total power production for one year is illustrated, for all scenarios, in Fig 8.3 b). It can be seen that the optimal power production, green bar, for S1-S4 is decreased as the wind power penetration is increased. This is likely a consequence from the decreased average electricity prices, where the model has chosen to bypass the steam turbine rather than producing electricity in it (see Fig 8.2). For scenario S5, which has the largest power production, the average electricity price is high, thus it is profitable to produce more electricity than required to fulfil the heat demand. This

was also analysed by studying the number of operating hours exceeding the heat demand, which rose up to 19 % for S5, but was less than 5 % for the other scenarios. The power production when only operating with the steam turbine, blue bars in Fig 8.3 b), is 30-40 % larger for all scenarios compared to the revenue optimised ones. For this case, the steam turbine is always in operation and its power production is, regardless of electricity price, increased in accordance with the heat demand. The larger electricity generation is thereby a result from it always utilising the steam turbine rather than bypassing it to fulfil the required heat demand.

From the last chart in Fig 8.3, c), it can be seen that the gas turbines' load fluctuates more often for scenarios S3-S5 when operating in a revenue optimised way, green bars. Furthermore, the difference is larger among the optimal scenarios than for the ones not utilising bypass, blue bars. The reason for the gas turbines' load fluctuations in the optimal setting is likely since it is more connected to match the electricity prices, which fluctuate more when the wind power penetration is increased. Even if the gas turbines are not operated at full load, the full bypass case use supplementary firing to fulfil the heat demand. Thus, the gas turbines are more connected to increase the load to profit from high electricity prices. In contrast, in the case of "No Bypass", the gas turbines' load is mainly altered to fulfil the heat demand. Only after increasing the gas turbine load to 100 %, supplementary firing is used to increase the plant output. To have fluctuating loads on the gas turbines is also connected to a higher maintenance cost since this frequent load change can lead to damage of the units, which would have impacted the revenue results if included in the study. However, as the total operating hours studied was 3544, the share of gas turbine load ramping was less than 10 % for all operating hours.

It should further be pointed out that the wind power generation for the reference scenario, 2016, and S1 is equivalent, see Tab 7.2. However, the results are quite different for the total yearly revenue in Fig 8.3 a), where S1 has a higher revenue for both optimal and no bypass operations. This might stem from predictions of the electricity prices at that wind power penetration level, which thus are overpredicted in the wind profile for S1. Yet, the operational patterns between 2016 and S1 are rather similar, see Fig 8.3 b-c). The reason for the similarity in yearly power production might be a result from that S1 has an increased share of bypass operations compared to 2016. However, the share of hours exceeding the heat demand was 6 % for S1 whereas only 1 % for 2016. Thus, the total plant output is similar for these cases.

The possibility of implementing thermal storage was investigated for the scenarios in Tab 7.2. By allowing the model to produce 10 % less, or more, than the actual heat demand, the amount of heat produced below and above the original demand were compared. This is illustrated in Fig 8.4, where the red bars represent the heat produced below the actual demand, and the green bars the amount of surplus heat produced.

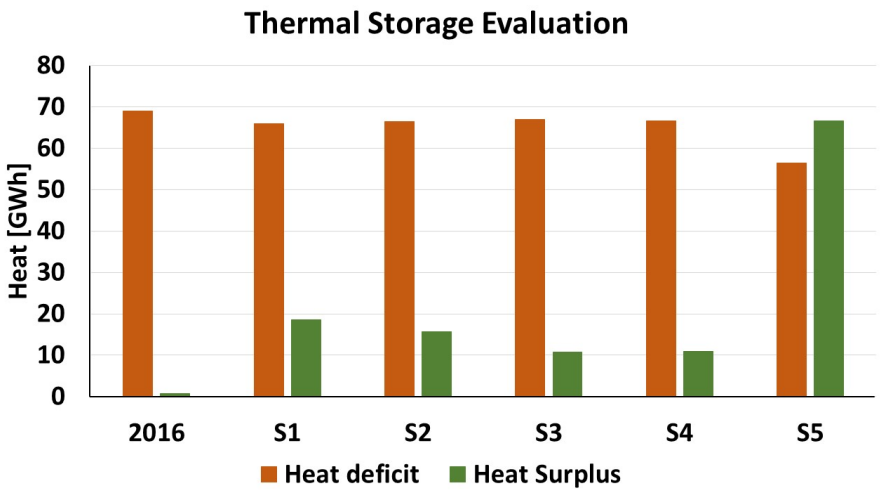


**Figure 8.4:** Comparison of heat deficit and heat surplus for the scenarios in Tab 7.2 when allowing the model to produce 10 % below the original heat demand.

From the evaluation in Fig 8.4, it was observed that neither 2016 nor scenarios S1-S4 fulfilled the heat demand when allowing the model to produce 10 % below the original demand. That is, the surplus heat produce did not cover the heat deficit operating hours. Therefore, the stored heat would not be able to cover the demand during hours with a deficit in heat production. Furthermore, when the electricity mix changes, S5, the number of high electricity price hours increases significantly, leading to more hours producing surplus heat. This heat could cover the heat deficit hours as the green bar is larger than the red one. A thermal storage tank enables storing heat produced during high electricity hours and use this during hours with low electricity price. The revenue could therefore increase the most in scenario S5 as it would allow the plant to decrease its production during unprofitable electricity price hours and still fulfil the heat demand throughout the year.

## 8.2 Sensitivity Analysis

A sensitivity analysis for an increased natural gas price is presented in Fig 8.5, where the green/red bars in Fig a) represent the yearly revenue and the black line shows share of operating hours utilising the direct condenser. In Fig 8.5 b), the black line illustrates the share of operating hours with full gas turbine load whereas the red one shows the share of hours with supplementary firing. The sensitivity analyses in the figures are conducted for the 2016 scenario in Tab 7.2.

(a)

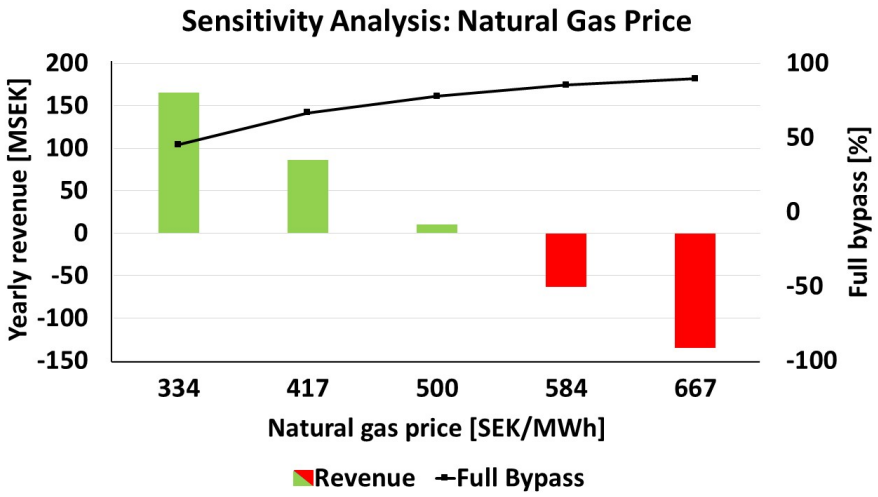


(b)

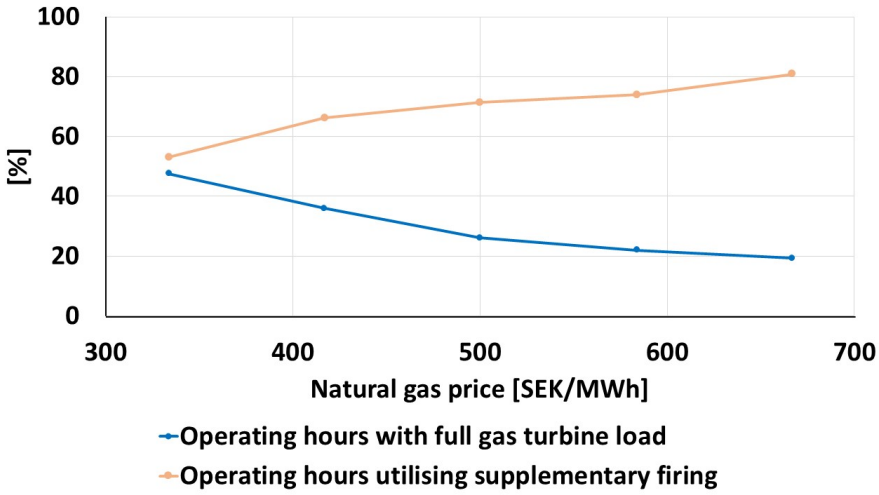


**Figure 8.5:** Sensitivity analysis of natural gas price [1] for the 2016 scenario where a) represents the yearly revenue change with increased fuel price, green/red bars, as well as the share of operating hours with full bypass, black line. Fig b) represents the share of operating hours with full gas turbine load, blue line, and the share of hours utilising supplementary firing, orange line.

The revenue decreases with an increased fuel price, where the breaking point is between 500-584 SEK/MWh. See Fig 8.5 a). Thus, a future increment of taxation for fossil fuels will have a significant impact on the profitability of a CCGT-CHP plant. However, seeing as the 2016 scenario might not represent future scenarios, S5 in Tab 7.2 was also studied in the same sensitivity analysis. This showed a similar trend for both graphs in Fig 8.5, but with a positive revenue at all fuel prices. That is, a future increase of natural gas price might not necessarily lead to a negative revenue for the operation of the CCGT-CHP plant. Yet, the fuel price has a significant impact on the plant's revenue and whether or not an increment will result in unprofitable operation is highly dependent on future energy systems.

In Fig 8.5 a) it can, from the black line, further be seen that the share of full bypass operations increases. This operational strategy utilises supplementary firing directly to fulfil the heat demand, and therefore avoids expensive fuel input shared between both heat and power in the steam turbine. That is, the heat demand is most profitably fulfilled via the direct condenser using heat from supplementary firing.

According to the sensitivity analysis in Fig 8.5 b), the operational pattern of the CCGT-CHP plant changes with the natural gas price. As the blue line illustrates, the operating hours with full gas turbine load decreases with an increased fuel price. This implies more hours with the gas turbines operating at part loads. Moreover, this reduces the total efficiency of the plant since the gas turbines' efficiency decreases with load. In contrast, as the fuel price increases, the use of supplementary firing is increased, orange line. This confirms the discussion above relating to full bypass utilisation and supplementary firing use. Furthermore, as the use of supplementary firing is restricted to the gas turbine load, it seems as the model selects the gas turbine load which allows it to have the desired supplementary firing input. This behaviour might not be found at an actual plant due to other operational limitations.

## 8.3 Project Discussion

The project's steps have been validated against historical data with rather high levels of conformity. Even though the linearised equations were based on a process model, and not the actual plant data, they resembled the reference plant at a satisfactory level. Furthermore, as the reference plant did not utilise steam turbine bypass during the reference year, this operating strategy could not have been implemented in the optimisation model if only reference data had been used in the linearisation. The use of software to develop a process model, linearised equations, and optimisation models is clearly a powerful tool when analysing alternative operating strategies for a CHP plant and could be applicable when evaluating new process configurations.

However, as the linearised models were derived for systems of gas turbines and supplementary firing combustors, the optimisation model could not differentiate how the separate units should be operated. Therefore, the results are on a plant level, where the suggested operating conditions might have changed if more detailed equations had been derived. However, as the reference data showed a similar operating pattern as the optimisation model with only the steam turbine alternative, the results should be valid on the level at which they were derived. Furthermore, the optimisation model only had the alternative to either utilise the steam turbine or fully bypass it. An improvement of the linearised equations would therefore be to allow the steam to be partly bypassed over the steam turbine.

Lastly, including aspects such as maintenance and operational costs, emission permits, and start-up costs would have given an even deeper understanding of which operational strategies are most profitable for a CHP plant in future energy system.

Furthermore, an analysis of how the plant's revenue relates to investment costs should be conducted to evaluate if the revenue is sufficient to cover annual fixed- and variable costs.

# 9
# Conclusion

This study investigates the value of measures for flexible operation of combined heat and power plants depending on power system scenarios. The work is based on a case study of a CCGT-CHP reference plant. The reference plant was mapped in 1) a steady-state process model using six off-design models based on heat and mass balances over the plant, and 2) through linearsation, using five linear equations with five factors, based on factorial design and linear regression. The linearised models were used to derive an optimisation model applying linear programming in which future energy scenarios' profitability and operations have been evaluated.

The developed process model reached a high level of conformity with the reference plant during steady-state operations. Furthermore, linearisation of multiple factors was crucial to accurately describe the plant's performance regarding power and heat outputs, fuel consumption, and supplementary firing utilisation. Moreover, the addition of actual process model data improved the linearised equations further. The main objective during validation was to achieve correlating trends between the outputs and reference data, where the trends correlated poorly when fewer factors were used to mathematically describe the plant. In conclusion, trend analysis proved sufficient in this context, since the validation showed a high conformity for both process model and linearised equations.

The operational strategy proposed by one of the optimisation models given historical power market data was close to the actual operation of reference plant for the reference year. For a power market scenario with volatile electricity prices (high share of non-dispatchable power), the results show that the flexibilisation strategy of steam turbine bypass and thermal storage is important to the operation of the plant. For one scenario studied, the yearly revenue increased with 24 % when steam turbine bypass was allowed (in operation 64 % of the operating hours). Thermal storage tanks are most feasible in an energy system without cheap base load technologies, such as nuclear power, where a large share of power production comes from variable renewables.

The study showed that, depending on fuel price and future energy system, it would be profitable to consider new operating strategies for the CCGT-CHP plant. With an increased fuel price, the revenues are higher when operating the plant for heat production. However, if the energy generation mix in the system is changed, the CCGT-CHP plant can have an important part in the electricity system as well. The profitability of decreasing the power-to-heat ratio as well as aspects of operational costs, other than fuel price, should be analysed further.

# Bibliography


[1] Statistiska centralbyrån (2017), *Prisutveckling på energi samt leverantörsbyten, andra kvartalet 2017*, Statistiska centralbyrån på uppdrag av Energimyndigheten, Örebro.

[2] UNFCCC (2015), *Paris Agreement*, United Nations, Paris.

[3] International Energy Agency, "$CO_2$-Emissions Statistics - An essential tool for analysts and policy makers", Available at: https://www.iea.org/statistics/co2emissions/ (accessed: 29 Jan 2019).

[4] Agora Energiewende (2017), *Flexibility in thermal power plants - With a focus on existing coal-fied power plants*, Angora Energiewende, Berlin.

[5] IEA (2011), *Harnessing Variable Renewables - A Guide to the Balancing Challenge*, International Energy Agency, Paris.

[6] Lund, R. Mathiesen, V.B (2015), "Large combined heat and power plants in sustainable energy systems", *Applied Energy*, vol. 142, pp. 389-395.

[7] Jonshagen, K. (2011), *MODERN THERMAL POWER PLANTS - Aspects on Modelling and Evaluation*, Lund University, Lund.

[8] Romanchenko, D. Odenberger, M. Göransson, L. Johnsson, F. (2017), "Impact of electricity price fluctuations on the operation of district heating systems: A case study of district heating in Göteborg, Sweden", *Applied Energy*, vol. 204, pp. 16-30.

[9] Gong, M. Werner, S. (2015), "Exergy analysis of network temperature levels in Swedish and Danish district heating systems", *Renewable Energy*, vol. 85, pp. 106-113.

[10] Byman, K. (2016), *Electricity production in Sweden*, Royal Swedish Academy of Engineering Sciences, Stockholm, Sweden.

[11] Puga, J.N. (2010), "The Importance of Combined Cycle Generating Plants in Integrating Large Levels of Wind Power Generation", *The Electricity Journal*, vol. 23, No. 7, pp. 33-44.

[12] Breeze, P. (2014), *Power Generation Technologies - 2nd Edition*, Elsevier Ltd., Oxford.

[13] IRENA (2018), *Global Energy Transformation: A Roadmap to 2050*, International Renewable Energy Agency, Abu Dhabi.

[14] Hannemann, F. Kehlhofer, R. Rukes, B. Stirnimann, F. (2009), *Combined-Cycle Gas & Steam Turbine Power Plants*, 3rd Edition, Pennwell Corporation, Tulsa.

[15] Elstatistik, (2019), "Nordic electricity production", available at: http://elstatistik.se/ (accessed: 25 Mars 2019).

[16] Savloa, T. Keppo, I. (2017), "International review of district heating and cooling", *Energy*, vol. 137, pp. 617-631.

[17] Rezaie, B. Rosen, M.A (2012), "District heating and cooling: Review of technology and potential enhancements", *Applied Energy*, vol. 93, pp. 2-10.

[18] Zhang, N. Cai, R. (2002), "The role of district heating in future renewable energy systems", *Energy*, vol. 35, No. 3, pp. 1381-1390.

[19] Gadd, H. Werner, S. (2013), "Daily heat load variations in Swedish district heating systems", *Applied Energy*, vol. 106, pp. 47-55.

[20] Rokka, M (2019), *Presentation during study visit at Rya Kraftvärmeverk*, Göteborg Energi, Gothenburg.

[21] Göteborg Energi (2019), "Fjärrvärmepriser", available at: https://www.goteborgenergi.se/foretag/fjarrvarme-kyla/fjarrvarmepriser (accessed: 26 Mars 2019).

[22] Varberg Energi (2019), "Prismodell fjärrvärme", available at: http://www.varbergenergi.se/foretag/tjanster/fjarrvarme/prismodell-fjarrvarme/ (accessed: 26 Mars 2019).

[23] Halmstads Energi och Miljö (2018), "Fjärrvärmepriser", available at: https://www.hem.se/sv/fjarrvarme-2/priser-2019 (accessed: 26 Mars 2019).

[24] Bolland, O. (2014), *Thermal power generation*, Norwegian University of Science and Technology, Trondheim.

[25] Hwang S.H. Kim T.S. (2005), "Part load performance analysis of recuperated gas turbines considering engine configuration and operation strategy", *Energy*, vol. 31, No. 2-3, pp. 260-277.

[26] Brun K. Kurz R (2001), "Degradation in Gas Turbine Systems", *Journal of Engineering for Gas Turbines and Power*, vol. 123, pp. 70-77.

[27] Savloa, T. Keppo, I. (2004), "Off-design simulation and mathematical modeling of small-scale CHP plants at part loads", *Applied Thermal Engineering*, vol. 25, No. 8-9, pp. 1219-1232.

[28] Genrup, M. Thern, M. (2018), *Ångturbinteknik, årsrapport 2019*, Energiforsk. Sweden.

[29] Polsky, M.P. (1982), *Sliding Pressure Operation in Combined Cycles*, ASME, Chicago, IL.

[30] Kavvadias, K. Jimenez Navarro, J.P. Zucker, A. (2017), *Case study on the impact of cogeneration and thermal storage on the flexibility of the power system*,

EUR 29082 EN, Publications Office of the European Union, Luxembourg, 2017, ISBN 978-92-79-77808-7, doi:10.2760/814708, JRC110285.

[31] Schröder, D. (2011), *Introducing Additional Heat Storage to the Hässelby CHP Plant - A case study on economic and ecological benefits achievable with heat storage in a deregulated electricity market*, KTH Industrial Engineering and Management, Stockholm, Sweden.

[32] Pym, a. welch, m. (2015), "improving the flexibility and efficiency of gas turbine-based distributed power plants", *POWER Engineering*, 14 september.

[33] WÄRTSILÄ (2019), "Combustion Engine vs Gas Turbine: Ramp Rate", available at: https://www.wartsila.com/energy/learning-center/technical-comparisons/combustion-engine-vs-gas-turbine-ramp-rate (accessed: 26 Mars 2019).

[34] Gobrecht, E. Ulma, A. Wechsung, M. Quinkertz,R. (2008), *USC Steam Turbine technology for maximum efficiency and operational flexibility*, Power-Gen Asia, Kuala Lumpur, Malaysia.

[35] Encabo Cáceres I. Montañés M.R. Nord O.L. (2018), "Flexible operation of combined cycle gas turbine power plants with supplementary firing", *Journal of Power Technologies*, vol. 98, No. 9, pp. 188-197.

[36] AIMday (2019), "Modelling & Simulation", available at: http://aimday.se/modelling-simulation/modelling-simulation/ (accessed: 26 Mars 2019).

[37] Zhang,G. Zheng, J. Xie, A. Yang, Y. Liu, L. (2016), "Thermodynamic analysis of combined cycle under design/off-design conditions for its efficient design and operation", *Energy Conversion and Management*, Vol. 126, pp. 76-88.

[38] Ganapathy V. (1990), "Simplify heat recovery steam generator evaluation", *Hydrocarbon Processing*, pp. 77.

[39] Song T.W. Kim J.H. Kim T.S. Ro S.T. (2001), "Performance prediction of axial flow compressors using stage characteristics and simultaneous calculation of interstage parameters ", *Proceedings of the Institution of Mechanical Engineers, Part A: Journal of Power and Energy*, vol. 215, pp. 89-98.

[40] Norberg, T. (2011), *Modeling of the steam system in a BWR*, Thesis Work, University of Uppsala, Uppsala.

[41] Steag ENERGY SERVICES, "EBSILON Professional for the design of power plants", available at: https://www.steag-systemtechnologies.com/en/products/ebsilon-professional/ (accessed: 28 Jan 2019).

[42] Murray-Smith, J.D. (2015), *Testing and Validation of Computer Simulation Models: Principles, Methods and Applications Simulation Foundations, Methods and Applications*, Springer, Switzerland.

[43] Montgomery, C.D. (2013), *Design and Analysis of Experiments*, 8th Edition, John Wiley & Sons, Inc., Arizona.

[44] Twomey, M.J. (1995), *Validation and Verification*, Department of Industrial and Manufacturing Engineering, Wichita State University, Kansas.

[45] Lythcke-Jørgensen (2016), *Design and optimization of flexible multi-generation systems*, Kgs. Luyngby: Technical University of Denmark (DTU), DCAMM Special Report No. S218.

[46] MathWorks®, (2019), "Linearize Nonlinear Models", available at: https://www.mathworks.com/help/slcontrol/ug/linearizing-nonlinear-models.html (accessed: 10 April 2019).

[47] GAMS, "An Introduction to GAMS", available at: https://www.gams.com/products/introduction/ (accessed: 28 Jan 2019).

[48] Statens energimyndighet (2017), *Vindkraftstatistik 2016 Nationell-, länsvis- och kommunal statistik*, Energimyndigheten, Eskilstuna.

[49] Naturvårdsverket (2019), *Minskad skattenedsättning av fossilt bränsle för persontransporter med inrikes sjöfart och för kraftvärmeproduktion*, WSP Sverige AB, Gothenburg.

# A

# Full Process Model

In Fig A.1, the full process model developed in EBSILON®Professional is shown. The model consists of three identical gas turbine and HRSG lines connected to one steam turbine system. Each line starts with a gas turbine, followed by a combustor for supplementary firing. The gas turbine's exhaust gases are heat exchanged in the HRSG through three super heaters, one evaporator, one feed water economiser, and finally with a district heating economiser. The three steam streams are mixed and enters a steam turbine, modelled as two sections. The steam is then condensed in two condensers before entering the feed water tank. The district heating consumption is modelled as a unit as well. The streams' colours are as follows:

- Brown = flue gases
- Orange = air
- Red = steam
- Blue = condensate/steam cycle water
- Dashed green/blue = district heating water

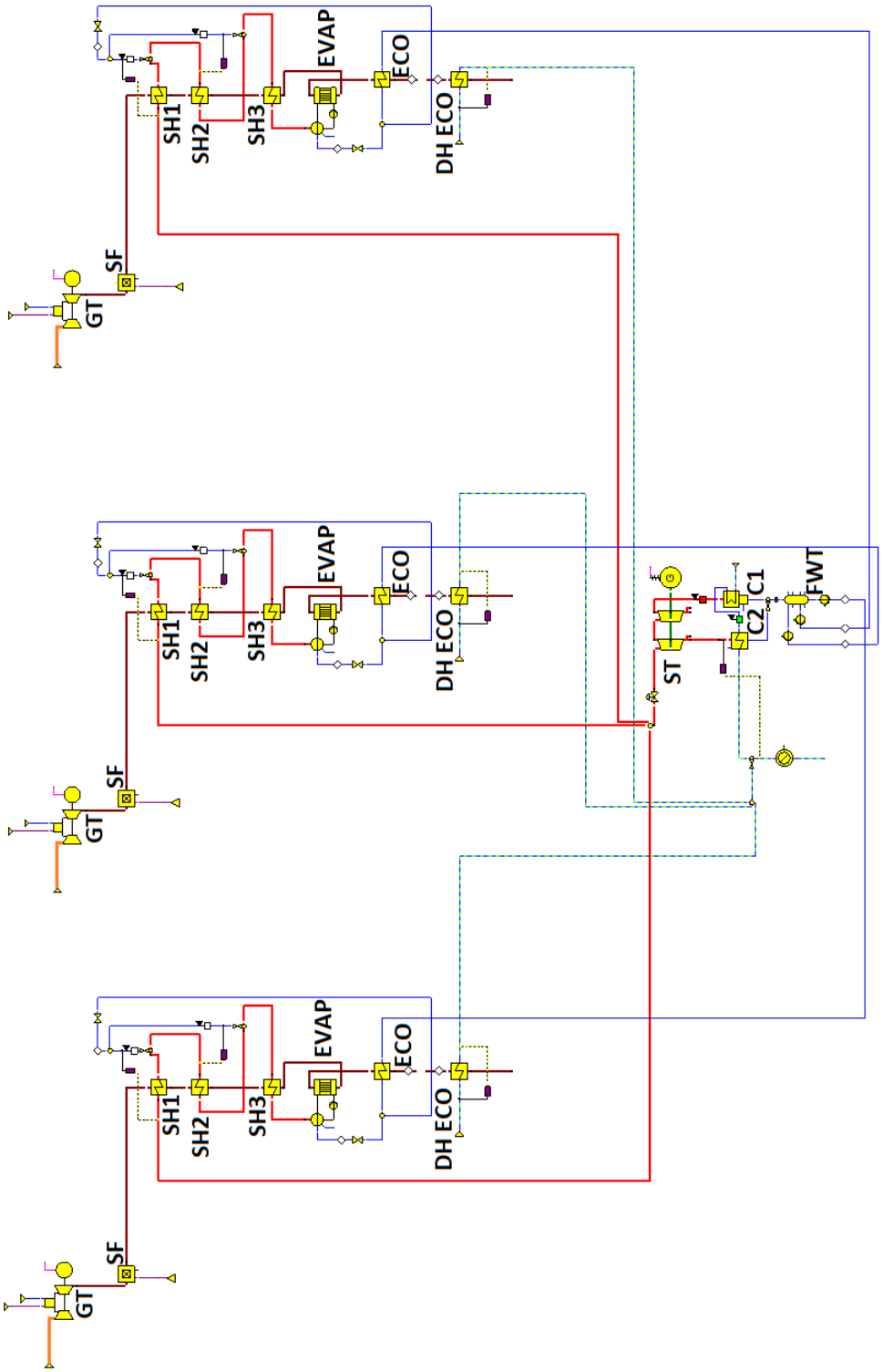


**Figure A.1:** Full process model of the CCGT-CHP plant.

In Tab A.1, the types of inputs given to the EBSILON®Professional-model are listed, as well as analysed outputs.

**Table A.1:** Inputs and outputs to/from model. The outputs presented are those studied from the process model.

| **Input** | **Output** |
|---|---|
| Gas turbine load | Gas turbine power |
| Ambient temperature | Steam turbine power |
| Ambient pressure | District heat |
| Supplementary firing fuel input | DH ECO heat |
| DHW target temperature after DH ECO | Stack temperature |
| DHW supply temperature | |
| DHW return temperature | |
| Intermediate temperature between COND 1 & COND 2 | |
| Evaporator pressure | |
| Feed water pressure | |
| Live steam temperature | |
| Steam turbine extraction pressure via DHW supply temperature | |

# Evaporator Area Estimation

Below follows a description of how the process model's evaporators' areas were calculated based on manufacturer drawings. From the drawings, the evaporator dimensions, number of tubes on the short side and tube diameter was known. This data was used to approximate the heat transfer area on the flue gas side, $A_{outside}$, to 3600 $m^2$ according to Eq A.1 and A.2

$$h_{evap} = d_{tube} n_{tuberows} + \delta_{tube}(n_{tuberows} + 1) \tag{A.1}$$

$$A_{outside} = l_{evap} o_{tubes} n_{tubes_{total}} \tag{A.2}$$

where $h_{evap}$ is the height of the evaporator, $d_{tube}$ tube diameter, $\delta_{tube}$ the spacing between the tubes, $n_{tubesrows}$ number of tubes rows, $l_{evap}$ evaporator length, $o_{tubes}$ tube perimeter and $n_{tubes_{total}}$ total number of tubes. Since the heat transfer is limited on the flue gas side, finned tubes are employed to increase the heat transfer. This is not accounted for in the calculations, why an underestimation of the heat transfer is expected. This is compensated for in the model by increasing the heat transfer coefficient on the flue gas side.

# B

# Process Model Validation

Below, the process model validations for off-design models with two gas turbines, B1-B3, are presented. Fig B.1 shows the comparison between the a) power and b) heat outputs from the process model and historical data, respectively.

**(a)**

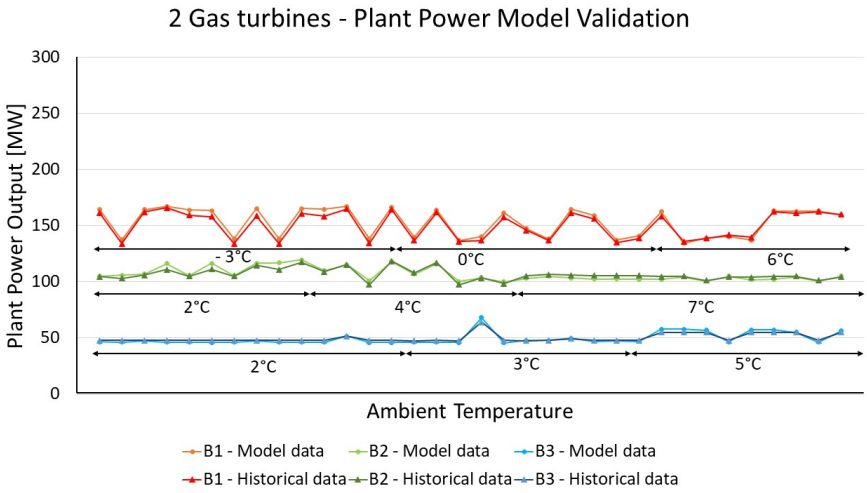


**(b)**

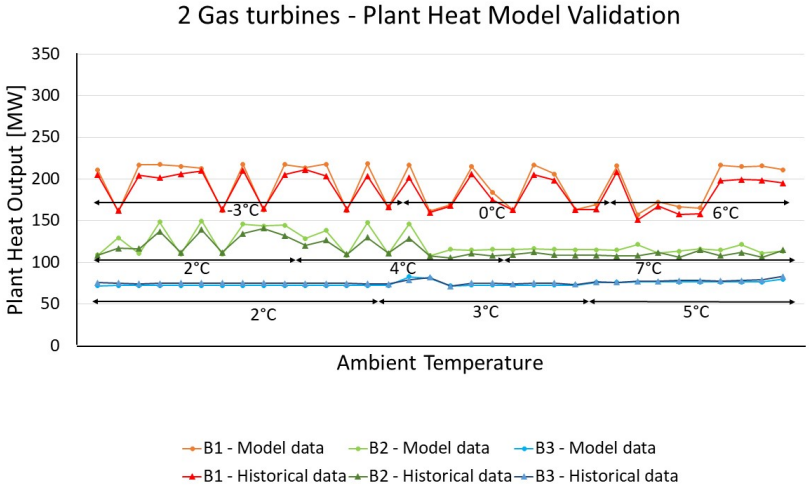


**Figure B.1:** Comparison between the historical data and process models' and a) power and b) heat output, with model names according to Tab 4.2. The black lines indicate the ambient temperature intervals studied in the process model validation.

In Fig B.2, the residual analyses for a) power and b) heat output are shown. The

residuals were calculated according to Eq 5.1.

**(a)**

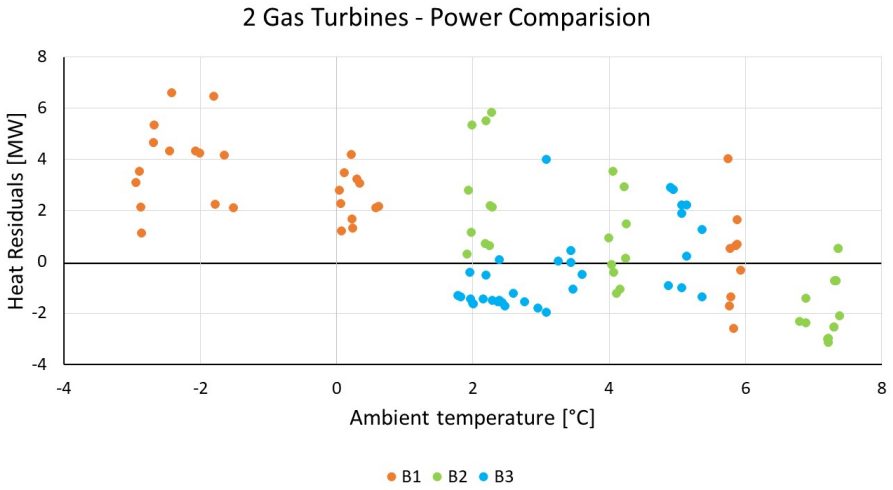


**(b)**

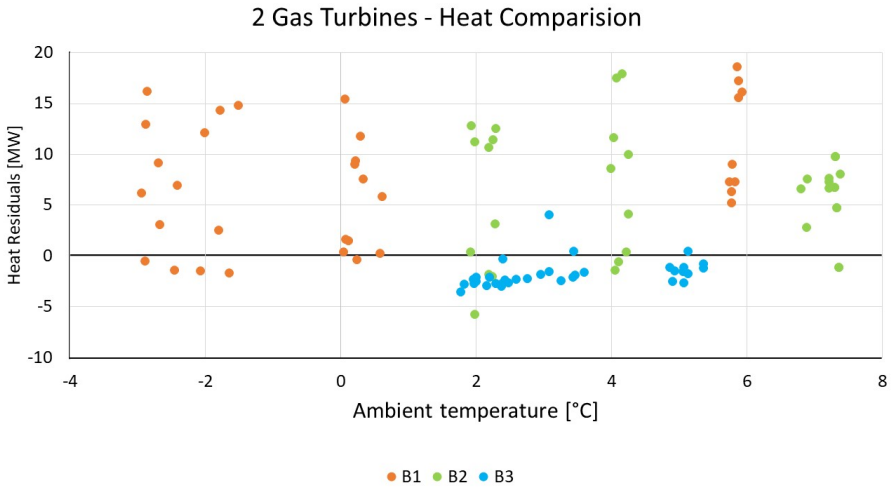


**Figure B.2:** Three off-design models' a) power and b) heat output residuals. Model names according Tab 4.2.

# C

# Validation of Linearised Model

The validation of the linerarised equations for scenarios without steam turbine bypass was performed graphically by comparing the model value with the process model value as well as analysing the percentage conformity. In Tab C.1, the starting and corrected average percentage conformity between model and equation values are shown, which were calculated according to Eq 5.2.

**Table C.1:** Percentage conformity comparison of the linerasied equations and the process model's heat and power output. The deviations when updating the factorial design is also presented.

| **Heat** | | | | | | |
|---|---|---|---|---|---|---|
| **Model** | A1 | A2 | A3 | B1 | B2 | B3 |
| **Start** | 0.99 | 0.95 | 0.73 | 1.00 | 0.97 | 0.84 |
| **Corrected** | 0.99 | 1.01 | 0.85 | 1.03 | 1.08 | 1.02 |
| **Power** | | | | | | |
| **Model** | A1 | A2 | A3 | B1 | B2 | B3 |
| **Start** | 0.99 | 1.00 | 0.90 | 1.04 | 1.06 | 1.00 |
| **Corrected** | 0.99 | 1.01 | 0.93 | 1.05 | 1.09 | 1.04 |

The corrected values are obtained after adding A3-values, both inputs and outputs, to the factorial design for both heat and power. In Tab C.1, it is clear that the A3-values have become better as they are closer to 1. However, both for heat and power, the deviation is still large. On the other hand, when correcting the equations, B1-B3 have gotten further from 1. This increase was deemed acceptable, as the other models were closer to 1. As can be seen from Tab C.1, both the heat and power equations are both under and overpredicted by the equations. Therefore, and improvement for one model would lead to a less accurate equation for another.

That the equations both under and overpredict the process model values can also be seen from the graphs in Fig C.1 and C.2. For example, in Fig C.1, the heat equation overpredicts the model's value for scenarios of A1, but underestimates for A3.

**(a)**

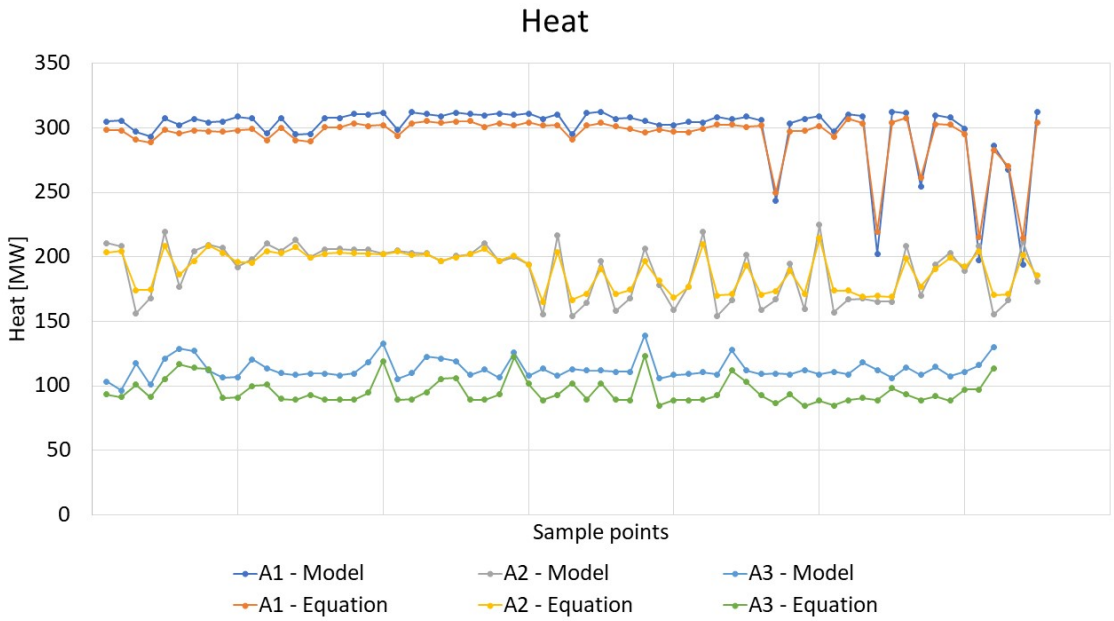


**(b)**

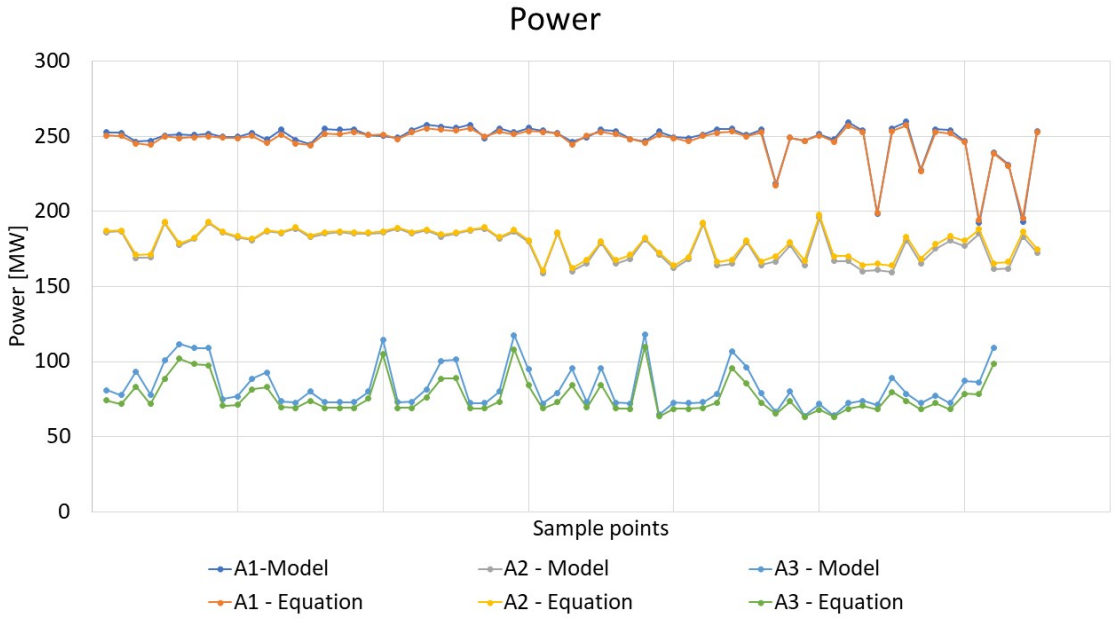


**Figure C.1:** Comparison between model output with three gas turbines, A1-A3, and equations for no bypass for a) heat and b) power. Model names according Tab 4.2.

**(a)**

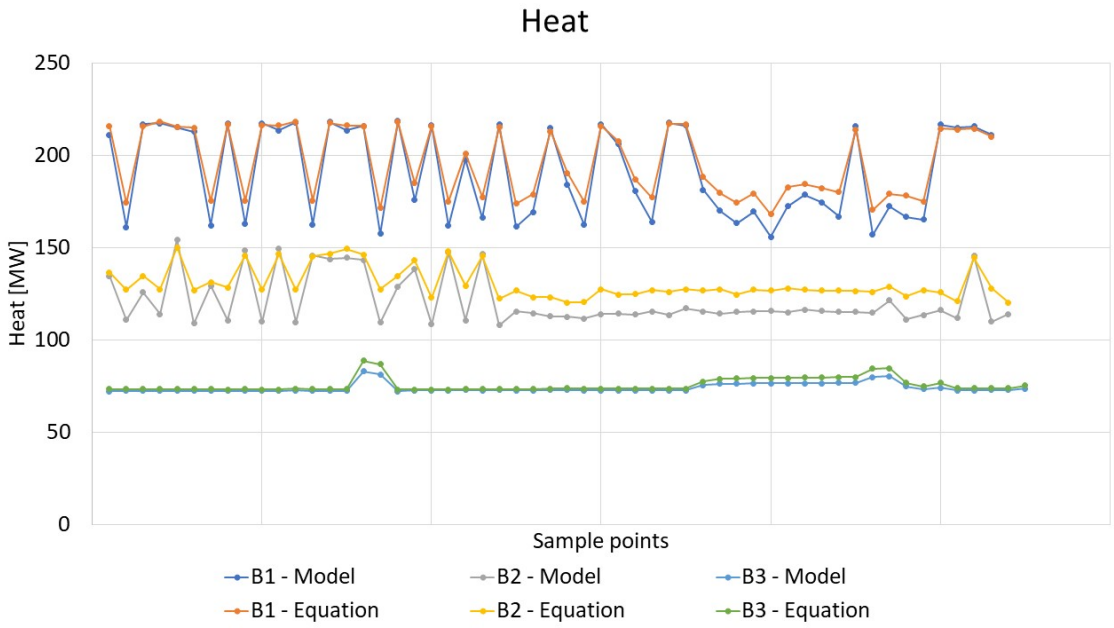


**(b)**

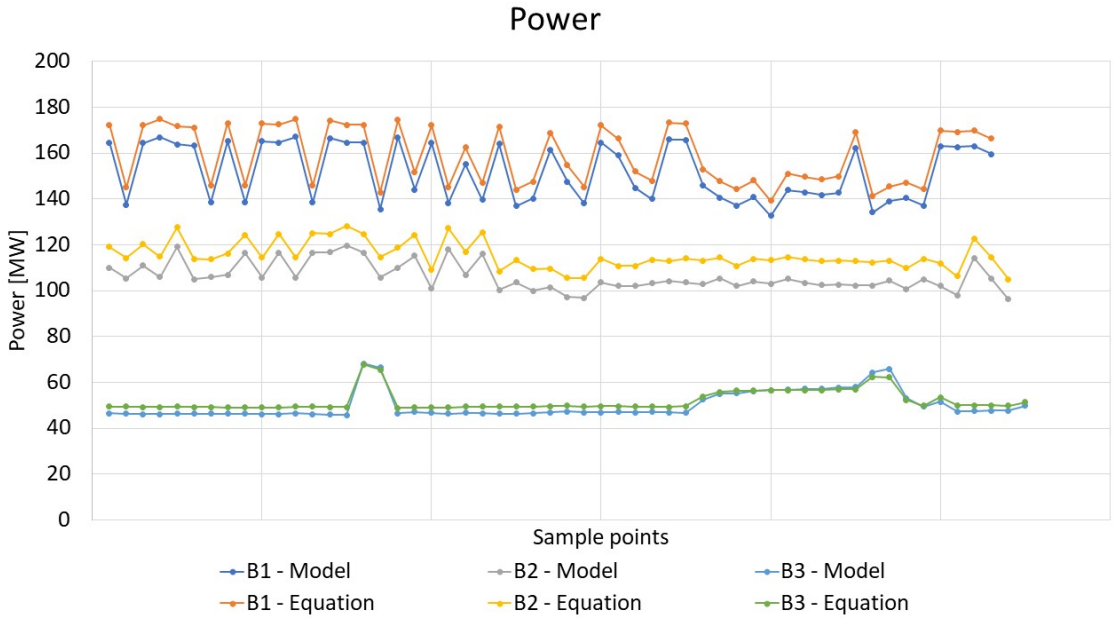


**Figure C.2:** Comparison between model output with two gas turbines, B1-B3, and equations for no bypass for a) heat and b) power. Model names according Tab 4.2.